Searching for long-lived particles beyond the Standard Model at the Large Hadron Collider

March 6, 2019

Particles beyond the Standard Model (SM) can generically have lifetimes that are long compared to SM particles at the weak scale. When produced at experiments such as the Large Hadron Collider (LHC) at CERN, these long-lived particles (LLPs) can decay far from the interaction vertex of the primary proton-proton collision. Such LLP signatures are distinct from those of promptly decaying particles that are targeted by the majority of searches for new physics at the LHC, often requiring customized techniques to identify, for example, significantly displaced decay vertices, tracks with atypical properties, and short track segments. Given their non-standard nature, a comprehensive overview of LLP signatures at the LHC is beneficial to ensure that possible avenues of the discovery of new physics are not overlooked. Here we report on the joint work of a community of theorists and experimentalists with the ATLAS, CMS, and LHCb experiments — as well as those working on dedicated experiments such as MoEDAL, milliQan, MATHUSLA, CODEX-b, and FASER — to survey the current state of LLP searches at the LHC, and to chart a path for the development of LLP searches into the future, both in the upcoming Run 3 and at the High-Luminosity LHC. The work is organized around the current and future potential capabilities of LHC experiments to generally discover new LLPs, and takes a signature-based approach to surveying classes of models that give rise to LLPs rather than emphasizing any particular theory motivation. We develop a set of simplified models; assess the coverage of current searches; document known, often unexpected backgrounds; explore the capabilities of proposed detector upgrades; provide recommendations for the presentation of search results; and look towards the newest frontiers, namely high-multiplicity “dark showers”, highlighting opportunities for expanding the LHC reach for these signals.

Editors:
Juliette Alimena[1] (Experimental Coverage, Backgrounds, Upgrades), James Beacham[2] (Document Editor, Simplified Models), Martino Borsato[3] (Backgrounds, Upgrades), Yangyang Cheng[4] (Upgrades), Xabier Cid Vidal[5] (Experimental Coverage), Giovanna Cottin[6] (Simplified Models, Reinterpretations), Albert De Roeck[7] (Experimental Coverage), Nishita Desai[8] (Reinterpretations), David Curtin[9] (Simplified Models), Jared A. Evans[10] (Simplified Models, Experimental Coverage), Simon Knapen[11] (Dark Showers), Sabine Kraml[12] (Reinterpretations), Andre Lessa[13] (Reinterpretations), Zhen Liu[14] (Simplified Models, Backgrounds, Reinterpretations), Sascha Mehlhase[15] (Backgrounds), Michael J. Ramsey-Musolf[16,126] (Simplified Models), Heather Russell[17] (Experimental Coverage), Jessie Shelton[18] (Simplified Models, Dark Showers), Brian Shuve[19,20] (Document Editor, Simplified Models, Simplified Models Library), Monica Verducci[21] (Upgrades), Jose Zurita[22,23] (Experimental Coverage)

Contributors & Endorsers:

Todd Adams[24], Michael Adersberger[25], Cristiano Alpigiani[26], Artur Apresyan[83], Robert John Bainbridge[27], Varvara Batozskaya[28], Hugues Beauchesne[29], Lisa Benato[30], S. Berlendis[31], Eshwen Bhal[32], Freya Blekman[33], Christina Borovilou[34], Jamie Boyd[7], Benjamin P. Brau[35], Lene Bryngemark[36], Oliver Buchmueller[27], Malte Buschmann[37], William Buttinger[7], Mario Campanelli[38], Cari Cesarotti[39], Chunhui Chen[40], Hsin-Chia Cheng[41], Sanha Cheong[42,43], Matthew Citron[44], Andrea Coccaro[45], V. Coco[7], Eric Conte[46], Félix Cormier[47], Louie D. Corpe[38], Nathaniel Craig[44], Yanou Cui[20], Elena Dall'Occo[48], C. Dallapiccola[35], M.R. Darwish[49], Alessandro Davoli[50,52], Annapaola de Cosa[51], Andrea De Simone[50,52], Luigi Delle Rose[53,54], Frank F. Deppisch[38], Biplab Dey[55], Miriam D. Diamond[9], Keith R. Dienes[31,56], Sven Dildick[57], Babette Döbrich[7], Marco Drewes[58], Melanie Eich[30], M. ElSawy[59,60], Alberto Escalante del Valle[61], Gabriel Facini[38], Marco Farina[62], Jonathan L. Feng[63], Oliver Fischer[22], H.U. Flaecher[32], Patrick Foldenauer[64], Marat Freytsis[65,11,66], Benjamin Fuks[67,68], Iftah Galon[69], Yuri Gershtein[70], Stefano Giagu[71], Andrea Giammanco[58], Vladimir V. Gligorov[72], Tobias Golling[73], Sergio Grancagnolo[74], Giuliano Gustavino[75], Andrew Haas[76], Kristian Hahn[77], Jan Hajer[58], Ahmed Hammad[78], Lukas Heinrich[7], Jan Heisig[58], J.C. Helo[79], Gavin Hesketh[38], Christopher S. Hill[1], Martin Hirsch[80], M. Hohlmann[81], W. Hulsbergen[48], John Huth[39], Philip Ilten[82], Thomas Jacques[50], Bodhitha Jayatilaka[83], Geng-Yuan Jeng[56], K.A. Johns[31], Toshiaki Kaji[84], Gregor Kasieczka[30], Yevgeny Kats[29], Malgorzata Kazana[85], Henning Keller[86], Maxim Yu. Khlopov[87,88], Felix Kling[63], Ted R. Kolberg[24], Igor Kostiuk[48,127], Emma Sian Kuwertz[7], Audrey Kvam[26], Greg Landsberg[89], Gaia Lanfranchi[90,7], Iñaki Lara[91], Alexander Ledovskoy[92], Dylan Linthorne[93], Jia Liu[94], Iacopo Longarini[95], Steven Lowette[33], Henry Lubatti[26], Margaret Lutz[35], Jingyu Luo[96], Judita Mamužić[80], Matthieu Marinangeli[97], Alberto Mariotti[33], Daniel Marlow[96], Matthew McCullough[7], Kevin McDermott[4], P. Mermod[73], David Milstead[98], Vasiliki A. Mitsou[80], Javier Montejo Berlingen[7], Filip Moortgat[7,99], Alessandro Morandini[50,52], Alice Polyxeni Morris[38], David Michael Morse[100], Stephen Mrenna[83], Benjamin Nachman[101], Miha Nemevšek[102], Fabrizio Nesti[103], Christian Ohm[104,105], Silvia Pascoli[106], Kevin Pedro[83], Cristián Peña[83,107], Karla Josefina Pena Rodriguez[30], Jónatan Piedra[108], James L. Pinfold[109], Antonio Policicchio[71], Goran Popara[110], Jessica Prisciandaro[58], Mason Proffitt[26], Giorgia Rauco[51], Federico Redi[97], Matthew Reece[39], Allison Reinsvold Hall[83], H. Rejeb Sfar[49], Sophie Renner[112], Amber Roepe[75], Manfredi Ronzani[76], Ennio Salvioni[113], Arka Santra[80], Ryu Sawada[114], Jakub Scholtz[106], Philip Schuster[42], Pedro Schwaller[112], Cristiano Sebastiani[71], Sezen Sekmen[115], Michele Selvaggi[7], Weinan Si[20], Livia Soffi[71], Daniel Stolarski[93], David Stuart[44], John Stupak III[75], Kevin Sung[77], Wendy Taylor[116], Sebastian Templ[61], Brooks Thomas[117], Emma Torró-Pastor[26], Daniele Trocino[99], Sebastian Trojanowski[118], Marco Trovato[119], Yuhsin Tsai[14], C.G. Tully[96], Tamás Álmos Vámi[120], Juan Carlos Vasquez[121], Carlos Vázquez Sierra[48], K. Vellidis[34], Basile Vermassen[99], Martina Vit[99], Devin G.E. Walker[122], Xiao-Ping Wang[119], Gordon Watts[26], Si Xie[107], Melissa Yexley[123], Charles Young[42], Jiang-Hao Yu[124,16], Piotr Zalewski[85], Yongchao Zhang[125]

[1] *Department of Physics, The Ohio State University, 191 W. Woodruff Ave., Columbus, OH 43210-1117, USA*
[2] *Department of Physics, Duke University, 120 Science Drive, Durham, NC 27710, USA*
[3] *Physikalisches Institut, Ruprecht-Karls-Universität Heidelberg, Im Neuenheimer Feld 226 69120, Heidelberg, Germany*
[4] *Cornell University, 245 East Avenue, Ithaca, NY 14853, USA*
[5] *Instituto Galego de Física de Altas Enerxías, U. Santiago de Compostela, IGFAE, Rúa de Xoaquín Díaz de Rábago, s/n, 15782 Santiago de*

Compostela, Spain
(6) *Department of Physics, National Taiwan University, Taipei 10617, Taiwan*
(7) *CERN, Esplanade des particules 1, Geneva, Switzerland*
(8) *Department of Theoretical Physics, Tata Institute of Fundamental Physics, Homi Bhabha Road, Mumbai 400005, India*
(9) *Department of Physics, University of Toronto, 60 St. George Street,Toronto, ON M5S 1A7, Canada*
(10) *Department of Physics, University of Cincinnati, 400 Geology/Physics Bldg., Cincinnati, OH 45221, USA*
(11) *School of Natural Sciences, Institute for Advanced Study, 1 Einstein Drive, Princeton, NJ 08540, USA*
(12) *Laboratoire de Physique Subatomique et de Cosmologie, Université Grenoble-Alpes, CNRS/IN2P3, 53 Avenue des Martyrs, F-38026 Grenoble, France*
(13) *Universidade Federal do ABC, Av. dos Estados, 5001, Santo Andre, 09210-580 SP, Brazil*
(14) *Maryland Center for Fundamental Physics, Department of Physics, University of Maryland, College Park, MD 20742, USA*
(15) *Faculty of Physics, Ludwig-Maximilians-Universität München, Schellingstraße 4, 80799 Munich, Germany*
(16) *Amherst Center for Fundamental Interactions, Department of Physics, University of Massachusetts Amherst, Lederle Graduate Research Center 416, Amherst, MA 01003 USA*
(17) *Department of Physics, McGill University, Montreal, QC H3A 2T8, Canada*
(18) *University of Illinois at Urbana-Champaign, 1110 W. Green St., Urbana, IL 61801, USA*
(19) *Harvey Mudd College, 301 Platt Blvd., Claremont, CA 91711, USA*
(20) *University of California, Riverside, 900 University Avenue, Riverside, CA 92521, USA*
(21) *Universita' di Roma Tre and INFN, via della Vasca Navale 84 00146 Roma Italy*
(22) *Institute for Nuclear Physics (IKP), Karlsruhe Institute of Technology, Hermann-von-Helmholtz-Platz 1, D-76344 Eggenstein-Leopoldshafen, Germany*
(23) *Institute for Theoretical Particle Physics (TTP), Karlsruhe Institute of Technology, Engesserstraße 7, D-76128 Karlsruhe, Germany*
(24) *Florida State University, 77 Chieftan Way, Tallahassee, FL 32306, USA*
(25) *Faculty of Physics, Ludwig-Maximilians Universität München, Schellingstrasse 4, 80799 Munich, Germany*
(26) *University of Washington, Seattle, 1410 NE Campus Parkway Seattle, WA 98195, USA*
(27) *High Energy Physics Group, Blackett Laboratory, Imperial College, Prince Consort Road, London SW7 2AZ, UK*
(28) *National Centre for Nuclear Research (NCBJ), Hoża 69, 00-681 Warsaw, Poland*
(29) *Department of Physics, Ben-Gurion University, 1 Ben-Gurion Boulevard Beer-Sheva, Beer-Sheva 8410501, Israel*
(30) *Institut für Experimentalphysik, Universität Hamburg, Luruper Chaussee 149, 22761 Hamburg, Germany*
(31) *University of Arizona, 118 E. 4th St., Tucson AZ 85721, USA*
(32) *University of Bristol, HH Wills Physics Laboratory, Tyndall Avenue, Bristol, BS8 1TL, UK*
(33) *IIHE, Vrije Universiteit Brussel, Pleinlaan 2, 1050 Brussels, Belgium*
(34) *Physics Department, National and Kapodistrian University of Athens, Panepistimioupoli, Zografou, 15784, Greece*
(35) *University of Massachusetts, Amherst, 1126 LGRT, University of Massachusetts, Amherst, MA 01003-9337, USA*
(36) *Department of Physics, Division of Particle Physics, Lund University, Box 118, 221 00 Lund, Sweden*
(37) *Leinweber Center for Theoretical Physics, University of Michigan, 450 Church Street, Ann Arbor MI-48109, USA*
(38) *University College London, Gower Street WC1E 6BT London, UK*
(39) *Department of Physics, Harvard University, 17 Oxford Street, Cambridge, MA, 02138*
(40) *Department of Physics and Astronomy, Iowa State University, 2323 Osborn Drive, Physics 0012, Ames, IA 50011-3160, USA*
(41) *Department of Physics, University of California, Davis, One Shields Avenue, Davis, CA 95616, USA*
(42) *SLAC National Accelerator Laboratory, 2575 Sand Hill Rd, Menlo Park, CA 94025, USA*
(43) *Physics Department, Stanford University, 450 Serra Mall, Stanford, CA 94305, USA*
(44) *Department of Physics, Broida Hall, University of California, Santa Barbara, CA 93106, USA*
(45) *INFN Sezione di Genova, Via Dodecaneso, 33 - 16146 - Genova, Italy*
(46) *Institut Pluridisciplinaire Hubert Curien (IPHC), Département Recherches Subatomiques, Université de Strasbourg/CNRS-IN2P3, 23 Rue du Loess, F-67037 Strasbourg, France*
(47) *Department of Physics & Astronomy, The University of British Columbia, 2329 West Mall, Vancouver, BC V6T 1Z4, Canada*
(48) *Nikhef National Institute for Subatomic Physics, Science Park 105, 1098 XG Amsterdam, The Netherlands*
(49) *Antwerp University, Prinsstraat 13, 2000 Antwerpen, Belgium*
(50) *SISSA, Via Bonomea 265, Trieste, 34136, Italy*
(51) *University of Zürich, Winterthurerstrasse 190, 8057 Zurich, Switzerland*
(52) *INFN Sezione di Trieste, via Bonomea 265, 34136 Trieste, Italy*
(53) *Department of Physics and Astronomy, University of Florence, Via G. Sansone 1, 50019 Sesto Fiorentino, Italy*
(54) *University of Southampton, Highfield, Southampton SO17 1BJ, UK*
(55) *Institute of Particle Physics, Central China Normal University, Wuhan, Hubei, China*
(56) *Department of Physics, University of Maryland, 4296 Stadium Drive, College Park, MD 20742, USA*
(57) *Texas A&M University, 4242 TAMU College Station, TX 77843-4242, USA*
(58) *Centre for Cosmology, Particle Physics and Phenomenology (CP3), Université catholique de Louvain, Chemin du Cyclotron 2, B-1348, Louvain-la-Neuve, Belgium*
(59) *Basic Science department, Faculty of Engineering, The British University in Egypt, El Sherouk City, Misr-Ismalia Road, Postal No 11837, PO Box 43, Cairo, Egypt*
(60) *Physics department, Faculty of Science, Beni Suef University, Qism Bani Sweif, Bani Sweif, Beni Suef Governorate, Egypt*
(61) *Institute of High Energy Physics, Austrian Academy of Sciences, Nikolsdorfer Gasse 18, 1050 Vienna, Austria*
(62) *Stony Brook University, Stony Brook, NY 11794-3840, USA*
(63) *Department of Physics and Astronomy, University of California, Irvine, CA 92697-4575, USA*
(64) *Institut für Theoretische Physik, Universität Heidelberg, Philosophenweg 16, D-69120 Heidelberg, Germany*
(65) *Raymond and Beverly Sackler School of Physics and Astronomy, Tel Aviv University, Tel-Aviv 69978, Israel*
(66) *Institute of Theoretical Science, University of Oregon, Eugene, OR 97403, USA*
(67) *Laboratoire de Physique Théorique et Hautes Energies (LPTHE), UMR 7589, Sorbonne Université et CNRS, 4 place Jussieu, 75252 Paris*

Cedex 05, France
[68] *Institut Universitaire de France, 103 boulevard Saint-Michel, 75005 Paris, France*
[69] *New High Energy Theory Center, Rutgers, The State University of New Jersey, Piscataway, NJ 08854-8019, USA*
[70] *Rutgers University, 136 Frelinghuysen Rd, Piscataway, NJ 08854 USA*
[71] *Sapienza Università di Roma and INFN Roma1, P.le A. Moro 5, Roma, 00185, Italy*
[72] *LPNHE, Sorbonne Université, Paris Diderot Sorbonne Paris Cité, CNRS/IN2P3, Barre 12-22, 4 Place Jussieu, 75252 Paris CEDEX 05, France*
[73] *Département de Physique Nucléaire et Corpusculaire, Université de Genève, 24, quai Ernest-Ansermet CH-1211 Genève 4, Switzerland*
[74] *Humboldt-Universität, Newtonstraße 15 12489 Berlin, Germany*
[75] *The University of Oklahoma, 440 W. Brooks St. Norman, OK 73019, USA*
[76] *New York University, 726 Broadway, New York, NY 10003, USA*
[77] *Northwestern University, 2145 Sheridan Rd, Evanston, IL 60208, USA*
[78] *Departement of Physics, University of Basel, Klingelbergstrasse 82, 4056, Basel, Switzerland*
[79] *Departamento de Física y Astronomía, Facultad de Ciencias, Universidad de La Serena, Avenida Cisternas 1200, La Serena, Chile*
[80] *Instituto de Física Corpuscular / Consejo Superior de Investigaciones Científicas - University of Valencia (IFIC / CSIC - UV), Carrer del Catedrátic José Beltrán Martinez, 2, 46980 Paterna, València*
[81] *Dept. of Aerospace, Physics & Space Sciences, Florida Institute of Technology, 150 W. University Blvd., Melbourne, FL 32901, USA*
[82] *University of Birmingham, Edgbaston, Birmingham B15 2TT, UK*
[83] *Fermi National Accelerator Laboratory, PO Box 500, Batavia, IL 60510*
[84] *Waseda University, Ookubo 3-4-1, Shinjuku-ku, Tokyo 169-8555, Japan*
[85] *National Centre for Nuclear Research (NCBJ), Andrzeja Sołtana 7, 05-400 Otwock-Świerk, Poland*
[86] *RWTH Aachen University, Otto-Blumenthal-Straße, 52074 Aachen, Germany*
[87] *National Research Nuclear University MEPHI, Kashirskoe chaussee 31, Moscow 115409, Russia*
[88] *APC Laboratory, 10, rue Alice Domon et Léonie Duquet 75205, Paris Cedex 13, France*
[89] *Brown University, 182 Hope St, Providence, RI 02912, USA*
[90] *Laboratori Nazionali di Frascati, INFN, via E. Fermi 40 00044 Frascati RM, Italy*
[91] *Instituto de Física Teórica (UAM-CSIC), C/Nicolás Cabrera 13-15 Campus de Cantoblanco 28049 Madrid, Spain*
[92] *Physics Department, University of Virginia, PO Box 400714, 382 McCormick Rd , Charlottesville, VA, 22904-4714, USA*
[93] *Carleton University, 1125 Colonel By Dr, Ottawa, ON K1S 5B6, Canada*
[94] *Enrico Fermi Institute, University of Chicago, 5640 S. Ellis Avenue, RI-183, Chicago, IL 60637, USA*
[95] *Università degli studi di Roma "La Sapienza" and INFN Roma, Dipartimento di Fisica G. Marconi. Piazzale Aldo Moro 5, 00185, Roma, Italy*
[96] *Physics Department, Washington Road, Princeton University, Princeton, NJ 08544, USA*
[97] *École Polytechnique Fédérale de Lausanne, Route Cantonale, 1015 Lausanne, Switzerland*
[98] *Fysikum, Stockholms Universitet, Roslagstullsbacken 21, 114 21 Stockholm, Sweden*
[99] *Department of Physics and Astronomy, University of Ghent, Proeftuinstraat 86, B-9000 Ghent, Belgium*
[100] *Northeastern University, 360 Huntington Ave., Boston, Massachusetts 02115, USA*
[101] *Physics Division, Lawrence Berkeley National Laboratory, Berkeley, 1 Cyclotron Road, CA 94720, USA*
[102] *Jožef Stefan Institute, Jamova 39, Ljubljana 1000, Slovenia*
[103] *Università dell'Aquila, via Vetoio, L'Aquila, 67100, Italy*
[104] *KTH Royal Institute of Technology, AlbaNova Universitetscentrum, KTH, Physics Department, SE-106 91 Stockholm, Sweden*
[105] *Oskar Klein Centre for Cosmoparticle Physics, Stockholm University, SE-106 91 Stockholm, Sweden*
[106] *IPPP, Department of Physics, Durham University, South Road, Durham, DH1 3LE, UK*
[107] *California Institute of Technology, 1200 E California Blvd, MC 256-48, Pasadena, CA, 91125, USA*
[108] *IFCA (CSIC - Universidad de Cantabria), Avenida de los Castros, 39005 Santander, Cantabria, Spain*
[109] *Physics Department, University of Alberta, Edmonton, AB T6G 2E1, Canada*
[110] *Ruder Bošković Institute, Bijenička cesta 54, 10000 Zagreb, Croatia*
[111] *Université catholique de Louvain, Place de l'université 1, 1348 Ottignies-Louvain-la-Neuve, Belgium*
[112] *PRISMA Cluster of Excellence & Mainz Institute for Theoretical Physics, Johannes Gutenberg University, Staudingerweg 7, 55128 Mainz, Germany*
[113] *Technical University of Munich, Physics Department, James-Franck-Strasse 1, 85748 Garching, Germany*
[114] *International Center for Elementary Particle Physics, The University of Tokyo, Hongo 7-3-1, Bunkyo-ku, Tokyo 113-0033, Japan*
[115] *Department of Physics, Kyungpook National University, 80 Daehakro, Bukgu, Daegu 41566, South Korea*
[116] *York University, 4700 Keele St, Toronto, ON M3J 1P3, Canada*
[117] *Lafayette College, 730 High St. Easton, PA 18042, USA*
[118] *Consortium for Fundamental Physics, School of Mathematics and Statistics, University of Sheffield, Hounsfield Road, Sheffield S3 7RH, UK*
[119] *Argonne National Laboratory, 9700 Cass Avenue, Lemont, IL 60439, USA*
[120] *Wigner Research Centre for Physics, Konkoly-Thege Miklós út 29-33, Budapest 1121, Hungary*
[121] *Universidad Técnica Federico Santa María, Avenida España 1680, Valparaiso, Chile, 2340000*
[122] *Department of Physics and Astronomy, Dartmouth College, Hanover, NH 03755 USA*
[123] *Lancaster University, Lancaster LA1 4YW, UK*
[124] *CAS Key Laboratory of Theoretical Physics, Institute of Theoretical Physics, Chinese Academy of Sciences, Beijing 100190, China*
[125] *Department of Physics and McDonnell Center for the Space Sciences, Washington University, St. Louis, MO 63130, USA*
[126] *T.-D. Lee Institute and School of Physics and Astronomy, Shanghai Jiao Tong University, 800 Dongchuan Road, Shanghai, 200240, China*
[127] *Institute for Nuclear Research of the National Academy of Sciences (KINR), 47 Nauky Avenue, 03680, Kyiv, Ukraine*

Contact editors: lhc-llp-admin@cern.ch

Contents

1 Introduction

Document editors: James Beacham, Brian Shuve

Particles in the Standard Model (SM) have lifetimes spanning an enormous range of magnitudes, from the Z boson ($\tau \sim 2 \times 10^{-25}$ s) through to the proton ($\tau \gtrsim 10^{34}$ years) and electron (stable).

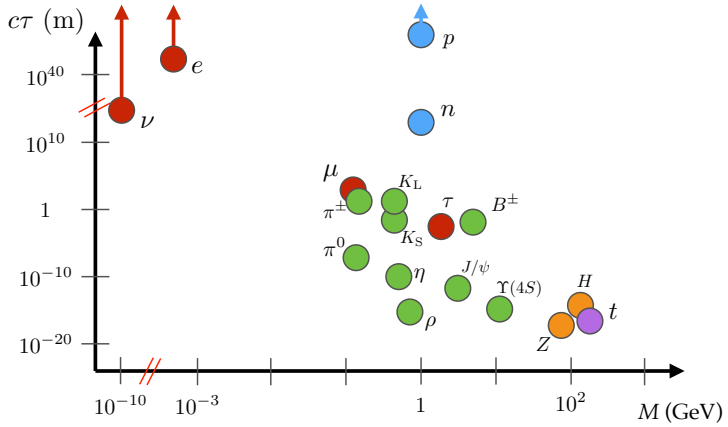

Figure 1.1: Particle lifetime $c\tau$, expressed in meters, as a function of particle mass, expressed in GeV, for a variety of particles in the Standard Model [1].

Similarly, models beyond the SM (BSM) typically predict new particles with a variety of lifetimes. In particular, new weak-scale particles can easily have long lifetimes for several reasons, including approximate symmetries that stabilize the long-lived particle (LLP), small couplings between the LLP and lighter states, and suppressed phase space available for decays. For particles moving close to the speed of light, this can lead to macroscopic, detectable displacements between the production and decay points of an unstable particle for $c\tau \gtrsim 10$ μm. [1]

The experimental signatures of LLPs at the LHC are varied and, by nature, are often very different from signals of SM processes. For example, LLP signatures can include tracks with unusual ionization and propagation properties; small, localized deposits of energy inside of the calorimeters without associated tracks; stopped particles that decay out of time with collisions; displaced vertices in the inner

[1] Recently, a comprehensive collection of the vast array of theoretical frameworks within which LLPs naturally arise has been assembled as part of the physics case document for the proposed MATHUSLA experiment [2]. Because the focus of the current document is on the experimental signatures of LLPs and explicitly not the theories that predict them, the combination of the MATHUSLA physics case document (and the large number of references therein) and the present document can be considered, together, a comprehensive view of the present status of theoretical motivation and experimental possibilities for the potential discovery of LLPs produced at the interaction points of the Large Hadron Collider.

detector or muon spectrometer; and disappearing, appearing, and kinked tracks.

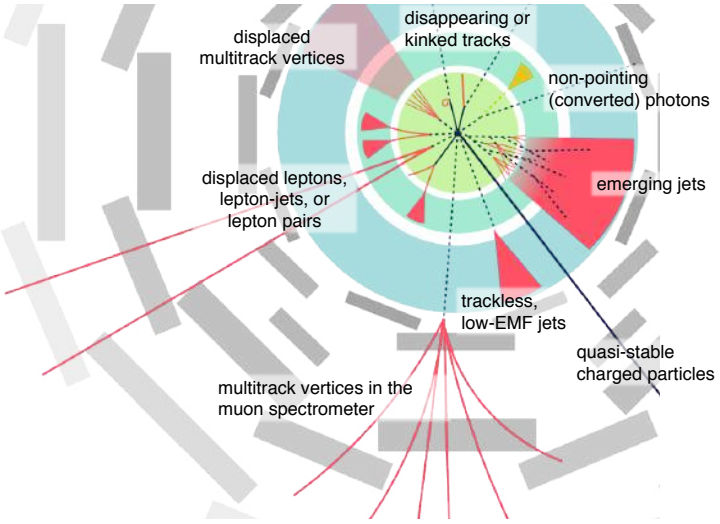

Figure 1.2: Schematic of the variety of challenging, atypical experimental signatures that can result from BSM LLPs in the detectors at the LHC. Shown is a cross-sectional plane in azimuthal angle, ϕ, of a general purpose detector such as ATLAS or CMS. From Ref. [3].

Because the long-lived particles of the SM have masses $\lesssim 5$ GeV and have well-understood experimental signatures, the unusual signatures of BSM LLPs offer excellent prospects for the discovery of new physics at particle colliders. At the same time, standard reconstruction algorithms may reject events or objects containing LLPs precisely because of their unusual nature, and dedicated searches are needed to uncover LLP signals. These atypical signatures can also resemble noise, pile-up, or mis-reconstructed objects in the detector; due to the rarity of such mis-reconstructions, Monte Carlo (MC) simulations may not accurately model backgrounds for LLP searches, and dedicated methods are needed to do so.

Although small compared to the large number of searches for prompt decays of new particles, many searches for LLPs at the ATLAS, CMS, and LHCb experiments at the Large Hadron Collider (LHC) have already been performed; we refer the reader to Chapter 3 for descriptions of and references to these searches. Existing LLP searches have necessitated the development of novel methods for identifying signals of LLPs, and measuring and suppressing the relevant backgrounds. Indeed, in several scenarios searches for LLPs have sensitivities that greatly exceed the search for similar, promptly decaying new particles (as is true, for example, for directly produced staus in supersymmetry [4]). The excellent sensitivity of these searches, together with the lack of a definitive signal in any prompt channels at the LHC, have focused attention on other types of LLP signatures that are not currently covered. These include low-mass LLPs that do not pass trigger or selection thresholds of current searches, high multiplicities of LLPs

produced in dark-sector showers, or unusual LLP production and decay modes that are not covered by current methods. Given the excellent sensitivity of LHC detectors to LLPs, along with the potentially large production cross sections of LLPs and the enormous amount of data expected to be collected when the LHC switches to high-luminosity running in the 2020s, it is imperative that the space of LLP signatures be explored as thoroughly as possible to ensure that no signals are missed. This is particularly important now, with the recent conclusion of LHC Run 2, as new triggering strategies for LLP signatures in the upcoming Run 3 can be investigated with urgency. Moreover, decisions are currently being made about detector upgrades for Phase 2 of the LHC, and design choices should be made to ensure that sensitivity to LLPs is retained or possibly improved through high-luminosity running, as may indeed be the case for many of the plans under consideration by the main experiments.

The increased interest in LLP signatures at the LHC is naturally complementary to the recognition that there are several BSM scenarios that give rise to particles difficult to optimally detect at the LHC — either promptly decaying particles or those with naturally long lifetimes — and that are searched for or planned to be searched for in fixed-target experiments, B-factories, and beam dump experiments [5–7].

The growing theoretical and experimental interest in LLPs has been mirrored by an increased activity in proposals for searches for LLPs produced at the main LHC interaction points — either within the existing ATLAS, CMS, and LHCb collaborations or with new, dedicated detectors — new experimental analyses, and meetings to communicate results and discuss new ideas. Workshops focused on LLPs at the University of Massachusetts, Amherst [2], in November of 2015; Fermilab; and KITP (UCSB) [3] in May of 2016, among others, highlighted the need for a community-wide effort to map the current space of both theoretical models for LLPs and the atypical experimental signatures that could be evidence of LLPs, assess the coverage of current experimental methods to these models, and identify areas where new searches are required. Additionally, the work presented in these meetings underscored the importance of presenting the results of experimental searches in a manner that allows for their application to different models, and generated new ideas for designing analyses with the goal of minimizing model dependence. Such largely model-independent presentation makes current searches more powerful by increasing their applicability to new scenarios, while reducing redundancies in searches and ensuring that gaps in coverage are identified and addressed. This task extends beyond the purview of any particular theoretical model or experiment, and requires an effort across collaborations to address the needs of the LLP community and illuminate a path forward.

This flurry of activity eventually coalesced in the establishment of a more central and regular platform — the LHC LLP Community

[2] "LHC Searches for Long-Lived BSM Particles: Theory Meets Experiment", https://www.physics.umass.edu/acfi/seminars-and-workshops/lhc-searches-for-long-lived-bsm%2Dparticles-theory-meets-experiment

[3] "Experimental Challenges for the LHC Run II", http://online.kitp.ucsb.edu/online/experlhc16/

— for experimentalists at the LHC and those in the theoretical and phenomenological communities to exchange ideas about LLP searches to ensure the full discovery potential of the LHC. This began with a mini-workshop at CERN in May of 2016 [4] and has continued with workshops in April of 2017 at CERN [5], October of 2017 at ICTP Trieste [6], May of 2018 again at CERN [7], and at Nikhef, in Amsterdam, in October of 2018 [8].

This is the work undertaken by the LHC LLP Community and presented in this document. Based on the most pressing needs identified by the community, we organize the work of this initiative into a few key realms:

- **Simplified models:** We seek to identify a minimal (but expandable) set of simplified models that capture, with a very limited number of free parameters, the most important LLP signatures motivated by theory and accessible at the LHC. The simplified models approach has been successfully applied to models such as supersymmetry (SUSY) and dark matter, and proposals exist for LLP simplified models in particular contexts. We aim to provide a basis of models that serves as a focal point for the other studies performed by the community, as well as a library that can be used in simulating LLP signal events, to allow for a common grammar to better understand how current and future searches cover LLP signature space.

- **Experimental coverage:** In spite of the many successful LLP searches undertaken by the ATLAS, CMS, and LHCb experiments, there remains a need for a systematic study of the complementary coverage of LLP searches to the parameter spaces of LLP models. Having developed a simplified model basis, we provide a comprehensive overview of the sensitivity of existing searches, highlighting gaps in coverage and high-priority searches to be undertaken in the future.

- **Backgrounds to LLP searches:** We provide a summary and analysis of backgrounds for LLP signals at the LHC, sources of which can be rare, unexpected, and largely irrelevant for searches for prompt BSM particles, and thus not fully well understood. We assemble the collected knowledge and experience of backgrounds to prior searches with the intention of providing insight into the opportunities and challenges of searching for LLP signatures.

- **Upgrades and triggering strategies:** We discuss the prospects for LLP searches with upgraded detectors for Phase 2 of LHC running, with a focus on how upgrades can offer new sensitivity to LLPs as well as mitigate the effects of pile-up. New opportunities for improving sensitivity of triggers and searches to LLPs are additionally presented for the upgrades planned for Run 3. This is tied to the crucial question of triggers for LLPs; we discuss the performance of current triggers for LLPs, as well as the

[4] "LHC Long-Lived Particle Mini-Workshop", https://indico.cern.ch/e/LHC_LLP_2016

[5] "Searches for long-lived particles at the LHC: First workshop of the LHC LLP Community", https://indico.cern.ch/e/LHC_LLP_April_2017

[6] "Searches for long-lived particles at the LHC: Second workshop of the LHC LLP Community", https://indico.cern.ch/e/LHC_LLP_October_2017

[7] "Searching for long-lived particles at the LHC: Third workshop of the LHC LLP Community", https://indico.cern.ch/e/LHC_LLP_May_2018

[8] "Searches for long-lived particles at the LHC: Fourth workshop of the LHC LLP Community", https://indico.cern.ch/e/LHC_LLP_October_2018

effects of future upgrades to the trigger system. Most importantly, we identify a few concrete upgrade studies that should be performed by the experiments that are of prime interest to the community.

- **Reinterpretation of LLP searches:** Due to the non-standard nature of the objects used in analyses, LLP searches are notoriously hard to reinterpret for models beyond those considered by the experimental collaborations. Designing searches and presenting search results in a way that is broadly applicable to current and yet-to-be-developed LLP models is crucial to the impact and legacy of the LLP search program. We discuss the reinterpretation of the LLP searches by means of concrete examples to illustrate specific challenges and, based on the lessons learned from this procedure, we provide recommendations on the presentation of LLP experimental search results.
- **Dark showers:** Current LLP search strategies have limited sensitivity to models where the LLPs are very soft, highly collimated, and come in large multiplicities, as can occur in models of dark-sector showers. We report on recent progress in theoretically parameterizing the space of dark-shower models and signatures, as well as experimental searches to uncover these signals.

Finally, we provide information about current and proposed experiments to search for LLPs at the LHC via dedicated detectors. These include the MoEDAL monopole search, the milliQan milli-charged particle experiment, the MATHUSLA surface detector for ultra-LLPs, the CODEX-b proposal for a new detector near LHCb, and the FASER proposal for a long, narrow detector located in the forward direction well downstream one of the collision points.

This is the first report of the LHC LLP Community initiative, and is expected to be followed by future reports as our collective understanding of these signatures as a means of discovering new physics at the LHC evolves.

2
Simplified Models Yielding Long-Lived Particles

Contents

Chapter editors: James Beacham, Giovanna Cottin, David Curtin, Jared Evans, Zhen Liu, Michael Ramsey-Musolf, Jessie Shelton, Brian Shuve

Contributors: Oliver Buchmueller, Alessandro Davoli, Andrea De Simone, Kristian Hahn, Jan Heisig, Thomas Jacques, Matthew McCullough, Stephen Mrenna, Marco Trovato, Jiang-Hao Yu

Long-lived particles (LLPs) arise in many well-motivated theories of physics beyond the SM, ranging from heavily studied scenarios such as the minimal supersymmetric SM (MSSM) [8–12] to newer theoretical frameworks such as neutral naturalness [13–15] and hidden sector dark matter [16–21]. Macroscopic decay lengths of new particles naturally arise from the presence and breaking of symmetries, which can be motivated by cosmology (such as dark matter and baryogenesis) [22–35], neutrino masses [36–49], as well as solutions to the hierarchy problem [13–15, 50–55]; indeed, LLPs are generically a prediction of new hidden sectors at and below the weak scale [56–64]. An extensive and encyclopedic compilation of

theoretical motivations for LLPs has already been performed for the physics case of the proposed MATHUSLA experiment [2], and we refer the reader to this document and the references therein for an in-depth discussion of theoretical motivations for LLPs. Given the large number of theories predicting LLPs, however, it is clear that a comprehensive search program for LLPs is critical to fully leverage the LHC's immense capability to illuminate the physics of the weak scale and beyond.

The simplified model framework has proven to be a highly successful approach to characterizing signals of beyond the SM (BSM) physics. Simplified models have driven the development of searches for new signatures at the LHC and allowed existing searches to be reinterpreted for many models beyond the one(s) initially targeted in the analysis. Comprehensive simplified model programs exist for scenarios featuring prompt decays of new particles [65–71] or dark matter produced at colliders [72–83]. Simplified models are so successful because the majority of search sensitivity is driven by only a few broad aspects of a given BSM signature, such as the production process, overall production rate, and decay topology. Meanwhile, the sensitivity of searches is typically insensitive to other properties such as the spin of the particles involved [84–87].

To extend the simplified model approach to LLP signatures in a systematic way, we develop a proposal for a set of simplified models which aims to ensure that experimental results can be characterized as follows: (i) *powerful*, covering as much territory in model space as possible; (ii) *efficient*, reducing unnecessary redundancy among searches; (iii) *flexible*, so that they are broadly applicable to different types of models; and (iv) *durable*, providing a common framework for Monte Carlo (MC) simulation of signals and facilitating the communication of results of LLP searches so that they may be applied to new models for years to come. We elaborate on these goals in Section 2.1. This framework helps illuminate gaps in coverage and highlight areas where new searches are needed, and we undertake such a study in Chapter 3. Our efforts build on earlier work proposing simplified model programs for LLPs motivated by particular considerations such as SUSY or dark matter (DM) [88–93].

In our work, we concentrate on establishing an initial basis of simplified models representative of theories giving rise to final states with one or two LLPs [1]. The simplified model approach is very powerful for LLP signatures: the typically lower backgrounds for displaced signatures allow searches to be highly inclusive with respect to other objects in the event or the identification of objects originating from the decay of an LLP. This enables a single analysis to have sensitivity to a wide variety of models for LLP production and decay.

We organize our simplified models in terms of **LLP channels** characterized by a combination of a particular LLP production

[1] Some models predict moderately higher LLP multiplicities, but the coverage of such signatures from 1-2 LLP searches is good provided the LLPs do not overlap in the detector. Our proposed simplified models are not, however, representative of high-multiplicity signatures such as dark showers (see Section 2.6 and Chapter 7).

mode with a particular decay mode. Because the production and decay positions of LLPs are physically distinct [2], it is often possible to factorize and consider separately their production and decay [3]. For each LLP channel, the lifetime of the LLP is taken to be a free parameter. We emphasize that the LLP channel defined here is *not* the same as an experimental signature that manifests in the detector: a single channel can give rise to many different signatures depending on where (or whether) [4] the LLP decays occur inside the detector, while a single experimental search for a particular signature could potentially cover many simplified model channels. In this chapter, we focus on the construction and simulation of a concrete basis of LLP simplified model channels; a partial mapping of existing searches into our basis of simplified models is discussed in Chapter 3, along with the highest-priority gaps in current coverage and proposals for new searches.

As discussed in the existing simplified model literature, simplified models have their own limited range of applicability [71, 79–81, 99]. For example, the presentation of search results in terms of simplified models often assume 100% branching fractions into particular final states. In a UV model where the LLP decays in a very large number of ways, none of the individual simplified model searches may be sufficient to constrain it. Similarly, if the LLP is produced in a UV model with other associated objects that spoil the signal efficiency (for example, the production of energetic, prompt objects collimated with the LLP such that the signal fails isolation or displacement criteria; this is particularly important for high-multiplicity or dark-shower scenarios, as discussed in Chapter 7), then the simplified model result does not apply and a more targeted analysis is required to cover the model. Nevertheless, the simplified models framework allows us to organize possible production modes and signatures in a systematic way and identify if there are any interesting signals or parts of parameter space that are missed by current searches.Therefore, we present a proposal for simplified models here with the understanding that there exist scenarios where UV models remain important for developing searches and presenting results.

The basis of simplified models presented here is a starting point, rather than a final statement. The present goal is to provide a set of simplified models that covers the majority of the best-motivated and simplest UV models predicting LLPs, which we outline in Section 2.2. Many of these contain singly and doubly produced LLPs (or in some cases, three-to-four relatively isolated LLPs, which are typically covered well by searches for $1-2$ LLPs) and so we restrict our simplified model proposal to cover these multiplicities. By design, simplified models do not include all of the specific details and subtle features that may be found in a given complete model. Therefore, the provided list is meant to be expanded to cover new or more refined models as the LLP-search program develops. For instance, extending the simplified model framework to separately

[2] Indeed, the decay position may be so far from the collision point that external detectors can also be used to search for ultra-long-lived neutral or milli-charged particles [94–98].

[3] In addition to production and decay, a third consideration is the propagation of particles through the detector. While neutral LLPs undergo straightforward propagation, states with electric or color charge (*e.g.*, SUSY *R*-hadrons), or particles with exotic charges such as magnetic monopoles or quirks, typically engage in a more complicated and often very uncertain traverse through the detector. This spoils the factorization of LLP production and decay. The subtleties related to LLPs with electric or color charge is discussed more in Section 2.4.3. A trickier question is how to best simulate such states: since LLPs with electric or color charge interact with the detector material, there must be an interface between the detector simulation software and the program implementing decay. This is discussed further in Section 2.5.2.

[4] The case of detector-stable particles is understood to be included in the simplified models by setting $c\tau \to \infty$. In this case there is manifestly no dependence on the decay mode. See Section 2.3.2 for further details.

treat final states with heavy-flavor particles is of great interest (in analogy with the prompt case [100–102]); see Section 2.6 for a discussion of this and other limitations of the current framework along with future opportunities for expansion. High-multiplicity signatures such as dark showers or emerging jets present different experimental and theoretical issues, which are discussed in Chapter 7. Finally, a broader set of simplified models may be needed to present the results of experimental searches and to allow ready application of experimental results to UV models of interest (see Chapter 6).

2.1 *Goals of the Present Simplified Model Framework*

The purpose of the simplified model framework is to provide a simple, common language that experimentalists and theorists can use to describe theories of LLPs and the corresponding mapping between models and experimental signatures. We therefore want our simplified model space to:

1. Use a minimal but sufficient set of models to cover a wide range of the best-motivated theories of LLPs;
2. Furnish a simple map between models and signatures to enable a clear assessment of existing search coverage and possible gaps;
3. Expand flexibly when needed to incorporate theories and signatures not yet proposed;
4. Provide a concrete MC signal event generation framework for signals;
5. Facilitate the reinterpretation of searches by supplying a sufficiently varied set of standard benchmark models for which experimental efficiencies can be provided for validation purposes.

Note that points #1 and #5 are somewhat in tension with one another: we wish to have a compact set of models that can be the subject of systematic study in terms of experimental signatures, but expressing experimental results in terms of only this set of simplified models may make it challenging to reinterpret experimental searches for UV models that are not precisely described by one of the simplified models. In this section, we prioritize having a minimal set of simplified models for the purpose of studying experimental coverages and generating new search ideas, while we defer a discussion of simplified models in the presentation and reinterpretation of search results to Chapter 6. [5]

In the remainder of this chapter, we construct a proposal for a minimal basis of simplified models for events with one or two LLPs. We begin with a discussion of the well-motivated UV theories that predict the existence of LLPs, and identify a set of umbrella models that yield LLPs in Section 2.2. We next identify the

[5] We note that, in general, more benchmark models may be needed for enabling reliable reinterpretation than the minimal set discussed here. An example where an extended set of simplified models is used can be seen in the heavy stable charged particle (HSCP) reinterpretation in Section 6.3.2 (Table 6.1).

relevant (simplified) production and decay modes for LLPs in Section 2.3, emphasizing that each channel for production and decay has a characteristic set of predictions for the number and nature of *prompt* accompanying objects (AOs) producing along with the LLP. In Section 2.4, we combine these production and decay modes into our simplified model basis set and highlight how different umbrella models naturally populate the various LLP channels. Section 2.5 and Appendix A present a framework and instructions for how the best-motivated simplified model channels can be simulated in Monte Carlo (MC) using a new model library provided in Appendix A. Finally, limitations of the existing framework, along with opportunities for its further development are outlined in Section 2.6.

2.2 *Existing Well-Motivated Theories for LLPs*

Here we provide a brief distillation of many of the best-motivated theories with LLPs into five over-arching categories, focusing in particular on those that give rise to single and double production of LLPs at colliders. We emphasize that each of these categories is a broad umbrella containing many different individual models containing LLPs; in many cases, the motivations and model details among theories within a particular category may be very different, but tend to predict similar types of LLPs. Additionally, the categories are not mutually exclusive, with several examples of UV models falling into one or more category. In all cases, long lifetimes typically arise from some combination of hierarchies of scales in interactions that mediate decays; small couplings; and phase space considerations (such as small mass splittings between particles or large multiplicities of final-state particles in a decay). Many of the broad theoretical motivations for LLPs have recently been summarized in the literature [2].

The UV umbrella models we consider are:

- **Supersymmetry-like theories (SUSY).** This category contains models with multiple new particles carrying SM gauge charges and a variety of allowed cascade decays. Here LLPs can arise as a result of approximate symmetries (such as R-parity [52, 103, 104] or indeed SUSY itself in the case of gauge mediation [105]) or through a hierarchy of mass scales (such as highly off-shell intermediaries in split SUSY [106], or nearly-degenerate multiplets [56, 57, 107], as in anomaly-mediated SUSY breaking [58]). Finally, models of SUSY hidden sectors such as Stealth SUSY [51] generically lead to LLPs. Our terminology classifies any non-SUSY models with new SM gauge-charged particles, such as composite Higgs or extra-dimensional models, under the SUSY-like umbrella because of the prediction of new particles above the weak scale with SM gauge charges. In this category, LLP production is typically dominated by SM gauge interactions, whether of the LLP itself or of a heavy parent particle that de-

cays to LLPs.

- **Higgs-portal theories (Higgs).** In this category, LLPs couple predominantly to the SM-like Higgs boson. This possibility is well motivated because the SM Higgs field provides one of the leading renormalizable portals for new gauge-singlet particles to couple to the SM, and the experimental characterization of the Higgs boson leaves much scope for couplings of the Higgs to BSM physics [108, 109]. The most striking signatures here are exotic Higgs decays to low-mass particles [110] (as in many Hidden Valley scenarios [59, 60]), which can arise in models of neutral naturalness [13, 14, 111] and DM [112], as well as in more exotic scenarios such as relaxion models [113]. The Higgs is also special in that it comes with a rich set of associated production modes in addition to the dominant gluon-fusion process, with vector-boson fusion (VBF) and Higgs-strahlung (VH) production modes allowing novel opportunities for triggering on and suppressing backgrounds to Higgs-portal LLP signatures. Indeed, in many scenarios where LLPs are produced in exotic Higgs decays, associated-production modes can be the only way of triggering on the event.

- **Gauge-portal theories (ZP).** This category contains scenarios where new vector mediators can produce LLPs. These are similar to Higgs models, although here the vector mediator is predominantly produced from $q\bar{q}$ initial states without other associated objects except for gluon initial-state radiation (ISR). Examples include models where both SM fermions and LLPs carry a charge associated with a new Z' (for a review, see Ref. [114]), as well as either Abelian or non-Abelian dark photon or dark Z models [115] in which the couplings of new vector bosons to the SM are mediated by kinetic mixing. Scenarios with LLPs coupled to new gauge bosons are well motivated by theories of DM, particularly models with significant self-interactions [116–118] and/or sub-weak mass scales [17, 18, 20, 119, 120].

- **Dark-matter theories (DM):** non-SUSY and hidden-sector DM scenarios are collected in this category, which encompasses models where the cosmological DM is produced as a final state in the collider process. Examples of multi-component DM theories include models of new electroweak multiplets [57, 121–123], strongly interacting massive particles (SIMPs) [124], inelastic dark matter [125–128], models with DM coannihilation partners [91, 129–134] (including scenarios where the coannihilation partners are out of chemical equilibrium, giving distinctly predictions for the relic abundance [135–138]), and non-thermal "freeze-in" scenarios [139–146]. In many of these models, the collider phenomenology and LLP lifetime can be tied to the DM relic abundance [128, 139, 147]. For LLPs decaying inside the detector, an important feature distinguishing this category from the Higgs and gauge scenarios above is that an explicit detector-level

signature of a dark matter candidate, *i.e.*, missing energy ($\not{E}_{\mathrm{T}}$), is a necessary and irreducible component [30, 59, 60, 93, 126, 128, 148–150].

- **Heavy neutrino theories (RHν):** the see-saw mechanism of SM neutrino mass generation predicts new right-handed neutrino (RHN) states [151–155]. If the RHNs have masses in the GeV to TeV range, they typically have a long lifetime and can be probed at the LHC [38, 43–45, 47, 48, 156–167]. Examples of well-motivated, UV-complete models with RHNs include the neutrino minimal SM (νMSM) [168, 169] and the left−right symmetric model [170–173]. Characteristic features of models in this category are LLPs produced singly via SM neutral- and charged-current interactions, and lepton-rich signatures in terms of prompt and displaced objects (often in association with quarks). For example, in extended scenarios like left−right symmetric models, production through new right-handed W and Z bosons can result in between one and four LLPs, and cascade decays between RHNs can lead to phenomena such as doubly displaced decays. Additionally, RHNs can be produced via Higgs decays [40, 41, 44, 163, 165, 174].

It is possible for a given model to fit into two or more of the umbrella UV model categories. For example, a SUSY theory with a stable lightest SUSY particle (LSP) could have the LSP serve as a dark matter candidate, while alternatively DM could be a new electroweak multiplet, giving rise to SUSY-like signatures [57, 121–123]. In other models featuring particles charged under a confining gauge group (such as "quirks" [175]), there can exist many production possibilities for the LLPs, including via the Higgs portal and the annihilation of new TeV-scale states (see, for example, Ref. [176]). Thus, the umbrella models should not be considered as exclusive categories, but rather as over-arching scenarios that motivate particular classes of signatures (such as new SM gauge-charged particles in the SUSY-like category, or presence of $\not{E}_{\mathrm{T}}$ in DM models).

In developing our simplified model framework below, we construct maps between these UV model categories and the simplified model channels to illuminate some of the best-motivated combinations of production and decay modes for LLPs. This allows us to focus on the most interesting channels and assess their coverage in Chapter 3.

2.3 *The Simplified Model Building Blocks*

As discussed above, production and decay can largely be factorized in LLP searches [6]. This allows us to specify the relevant production and decay modes for LLP models separately; we then put them together and map the space of models into the umbrella categories of motivated theories.

[6] Once again, we comment that non-factorization of production and decay due to LLP interaction with the detector material and non-trivial propagation effects arise in models with LLPs with electric or color charge, and we discuss these subtleties further in Section 2.5.2

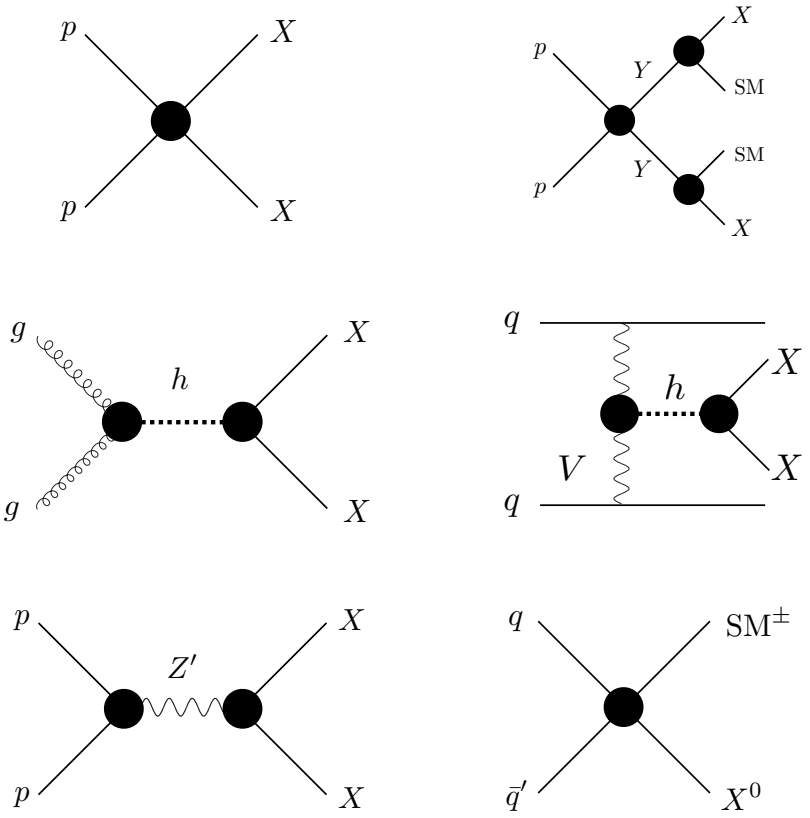

Figure 2.1: Schematic illustrations of LLP production modes in our simplified model framework. From top to bottom and left to right: direct pair production (DPP); heavy parent (HP); Higgs modes (HIG), including gluon fusion and VBF production (not shown here is VH production); heavy resonance (RES); charged current (CC).

2.3.1 *Production Modes*

Motivated by our over-arching UV frameworks, we can identify a minimal set of interesting production modes for LLPs. Schematic diagrams for each production mode are shown in Figure 2.1. These production modes determine LLP signal rates both by relating the LLP production cross section to meaningful theory parameters such as gauge charges or Higgs couplings, and by determining the kinematic distribution of the LLP. Additionally, a given production mechanism also makes clear predictions for the number and type of *prompt* objects accompanying the LLP(s). These prompt AOs can be important for both triggering on events with LLPs and for background rejection, particularly when the LLP has a low mass or decays purely hadronically, and they can be either SM states (leptons, $\not{E}_T$, tagging jets) or BSM objects such as Z' or dark photons [150, 177, 178].

- **Direct-Pair Production (DPP):** here the LLP is dominantly pair-produced non-resonantly from SM initial states. This is most straightforwardly obtained when the LLP is charged under a

SM gauge interaction. In this case, an irreducible production cross section is then specified by the LLP gauge charge and mass. Such continuum DPP can also occur in the presence of a (heavy, virtual) mediator (*e.g.*, an initial quark−antiquark pair may exchange a virtual squark to pair produce bino-like neutralinos); in this case the production cross section is essentially a free parameter, as it is determined by the unknown heavy mediator masses and couplings.

- **Heavy Parent (HP):** the LLP is produced in the decays of on-shell heavy-parent particles that are themselves pair produced from the pp initial state. The production cross section is essentially a free parameter, and is indirectly specified by the gauge charges and masses of the heavy parent particles. Heavy-parent production gives very different kinematics for the LLP than DPP, and often produces additional prompt AOs in the rapid cascade decays of the parents.

- **Higgs (HIG):** here the LLP is produced through its couplings to the SM-like Higgs boson. This case has an interesting interplay of possible production modes. The dominant production is via gluon fusion, which features no AOs beyond gluon ISR. Owing to its role in electroweak symmetry breaking, however, the Higgs has associated production modes (VBF, VH), each with its own characteristic features. The best prospects for discovery are for LLP masses below $m_h/2$, in which case the LLPs can be in decays of the on-shell SM-like Higgs boson. Higher-mass LLPs can still be produced via an off-shell Higgs, albeit at substantially lower rates [26, 179]. The LLP can be pair produced or singly produced through the Higgs portal depending on the model; an LLP X can also be produced in association with $\not{E}_{\mathrm{T}}$ via $h \to XX + \not{E}_{\mathrm{T}}$ or $h \to X + \not{E}_{\mathrm{T}}$. The cross section (or, equivalently, the Higgs branching fraction into the LLP) is a free parameter of the model. The Higgs mass can also be taken as a free parameter: there exist many theories that predict new exotic scalar states (such as the singlet-scalar extension to the SM [112]), and these new scalars can be produced in the same manner as the SM Higgs.

- **Heavy Resonance (RES):** here the LLP is produced in the decay of an on-shell resonance, such as a heavy Z' gauge boson initiated by $q\bar{q}$ initial state. Note that production via an off-shell resonance is kinematically similar to the DPP mode. As with HIG, the LLP can be pair produced or singly produced (potentially in association with $\not{E}_{\mathrm{T}}$). In RES models, ISR is the dominant source of prompt AOs. Models with new heavy scalars could conceivably fall into either RES or HIG; the main determining factor according to our organizational scheme is whether the scalar possesses Higgs-like production modes such as VBF and VH. Note that heavy resonance decays to SM particles also occur

in these models, and searches for such resonances [180–186] may complement the sensitivity for decays to LLPs.

- **Charged Current (CC):** in models with weak-scale right-handed neutrinos, the LLP can be produced in the leptonic decays of W/W'. Single production is favored. Prompt charged leptons from the charged-current interaction are typical prompt AOs.

It is important to note that each of the above production mechanisms has its own "natural" set of triggers to record the signal. For example, HIG production can be accompanied by forward jets or leptons that are characteristic of VBF or VH production. Similarly, CC production often results in prompt charged leptons, while HP production comes with AOs from the heavy-parent decay. However, the reader should be cautioned that this does not necessarily mean that the "natural" trigger is *optimal* for a particular signal. For example, the HIG modes suggest the use of VBF- or VH-based triggers, but if the LLP decays leptonically, it might be more efficient to trigger on the lepton from the LLP decay. Thus, the final word on which trigger is most effective for a given simplified model depends on the production mode as well as the nature and kinematics of the LLP decay. The prompt AOs of each production mode could still, however, be used to extend sensitivity to the model (see Section 6.3).

We also comment that some models may span several production modes. For example, a charged LLP that is part of an electroweak multiplet and nearly degenerate with a stable, neutral component [56–58, 92, 121–123, 187, 188] gives both DPP signatures (via $pp \to \chi^+\chi^-$) and CC production (via associated production $pp \to \chi^\pm\chi^0$). Comprehensive coverage of each of the above production modes will allow for a conservative determination of sensitivity for models that span many production modes.

2.3.2 *Decay Modes*

We now list a characteristic set of LLP decay modes. As we attempt to construct a minimal, manageable set of decay-mode building blocks, it is important to bear in mind that a given experimental search for LLPs can frequently be sensitive to a variety of possible LLP decay modes. As a result, it is not always necessary to perform separate searches for each possible decay mode as might otherwise be needed for prompt signatures.

The fact that LLP searches can be sensitive to many LLP decay modes is, in part, because LLPs that decay far from the collision point offer fewer avenues for particle identification. For example, for an LLP decaying inside of the calorimeter, most decay products are reconstructed as missing energy, or an energy deposition in the calorimeter. Consequently, particle identification criteria are typically relaxed in comparison to requirements on searches without displaced objects. Indeed, these "loose" collider objects can differ

significantly from the corresponding "tight", prompt objects. This leads to more inclusive analyses that can cover a wider range of signatures with a single search.

Additionally, backgrounds for LLP searches are often small; for a comprehensive discussion of backgrounds to LLP searches, see Chapter 4. As a result, tight identification and/or reconstruction criteria typically found in exclusive prompt analyses are no longer needed to suppress backgrounds. For example, ATLAS has a displaced vertex search sensitive to di-lepton and multi-track vertices that is relatively inclusive with respect to other objects originating from near the displaced vertex [189]. Similarly, CMS has an analysis sensitive to events with one each of a high-impact-parameter muon and electron without reconstructing a vertex or any other objects [190]. For these examples, the backgrounds are sufficiently low that other requirements may be relaxed and the specific decay mode of the LLP may not be too important so long as certain objects (such as muons) are present or the decay occurs in a specific location. An even more extreme example in this regard is the search for highly-ionizing tracks sensitive to electrically and color-charged LLPs. While the searches are primarily targeted to detector-stable particles (heavy stable charged particles or R-hadrons) they can also be used to probe intermediate lifetimes for which only a certain fraction of LLPs traverse the tracker before decaying (see *e.g.* [135]). Both because of low backgrounds as well as modified particle identification criteria compared to prompt searches, LLP searches can often be inclusive and therefore covered by a more limited range of simplified models.

In some cases, however, the topology of a decay does matter. One potentially important factor that influences the sensitivity of a search to a particular model is whether the LLP decays into two SM objects vs. three, because the kinematics of multi-body decay are distinct from two-body decay and this may affect the acceptance of particular search strategies. An additional simplified model featuring a three-body decay of the LLP may consequently be needed to span the space of signatures.

Below, we describe an irreducible set of decay modes that can be used to characterize LLP signatures for various LLP charges (including neutral, electrically charged, and color charged). For each, we also provide an explicit example for how the decay would appear in a particular UV model. **We emphasize that the following decay modes are loosely defined with the understanding that their signatures are also representative of similar, related decay modes; for example $2j$ or $2j + \not{E}_{\mathrm{T}}$ can also be proxies for $3j$ because searches for multi-body hadronic LLP decays can be sensitive to both and typically do not require reconstruction of a third jet.** It should also be noted that we are not recommending searches to be optimized to the exact, exclusive decay mode because that could suppress sensitivity to related but slightly more complicated LLP decays.

- **Di-photon decays:** the LLP can decay resonantly to $\gamma\gamma$ (like in Higgs-portal models or left−right symmetric models [191]) or to $\gamma\gamma$ + invisible (in DM models). This latter mode stands as a proxy for other $\gamma\gamma + X$ decays where the third object is not explicitly reconstructed, although whether X is truly invisible can influence the triggers used. *Example: a singlino decaying to a singlet (which decays to $\gamma\gamma$) and a gravitino in Stealth SUSY [51].*

- **Single-photon decays:** the LLP decays to γ + invisible (like in SUSY models). The SUSY model mandates a near-massless invisible particle, while other models (such as DM theories [127, 149]) allow for a heavy invisible particle. *Example: a bino decaying to photon plus gravitino in gauge-mediated models of SUSY breaking [192].*

- **Hadronic decays:** the LLP can decay into two jets (jj) (like in Higgs and gauge-portal models, or RPV SUSY), jj + invisible (SUSY, dark matter, or neutrino models), or j + invisible (SUSY). Here, "jet" (j) means either a light-quark parton, gluon, or b-quark. This category also encompasses decays directly into hadrons (for example, LLP decay into π^+ plus an invisible particle [56–58]). *Example: a scalar LLP decaying to $b\bar{b}$ due to mixing with the SM Higgs boson, as in models of neutral naturalness [13, 14, 111].*

- **Semi-leptonic decays:** the LLP can decay into a lepton + 1 jet (such as in leptoquark models) or 2 jets (like in SUSY or neutrino models). *Example: a right-handed neutrino decaying to a left-handed lepton and an on- or off-shell hadronically decaying W boson (or W' boson in a left−right symmetric model) [156].*

- **Leptonic decays:** the LLP can decay into $\ell^+\ell^-$(+invisible), or $\ell^\pm$ + invisible (as in Higgs-portal, gauge-portal, SUSY, or neutrino models). Here the symbol ℓ may be any flavor of charged lepton, but the decays are lepton flavor-universal and (for $\ell^+\ell^-$ decays) flavor-conserving. *Example: a wino decaying to a neutralino and an on- or off-shell leptonic Z boson in SUSY [52].*

- **Flavored leptonic decays:** the LLP can decay into ℓ_α + invisible, $\ell_\alpha^+\ell_\beta^-$ or $\ell_\alpha^+\ell_\beta^-$ + invisible where flavors $\alpha \neq \beta$ (as in SUSY or neutrino models). *Example: a neutralino decaying to two leptons and a neutrino in R-parity-violating SUSY [52]; or a right-handed neutrino decaying to two leptons and a neutrino [193].*

In all cases, both the LLP mass and proper lifetime are free parameters. Therefore, the case of detector-stable particles is automatically included by taking any of the above decay modes and taking the lifetime to infinity [7]. We emphasize that, depending on the location of the LLP within the detector, these decay modes may or may not be individually distinguishable: a displaced di-jet decay will look very different from a displaced di-photon decay in the tracker, but nearly identical if the decay occurs in the calorimeter. The goal

[7] As mentioned earlier, in the $c\tau \to \infty$ limit the decay mode becomes irrelevant. However, an exception is the search for particles that are stopped inside the detector material and decay out of time, which are discussed in Section 3.5.3.

here is to identify promising channels (as distinct from detector signatures).

As an example of how the above-listed decay modes cover the most important experimental signatures, we consider a scenario of an LLP decaying to top quarks. This scenario is very well motivated (for instance, with long-lived stops in SUSY) and might appear to merit its own decay category of an LLP decaying to one or more top quarks. However, the top quark immediately decays to final states that *are* covered in the above list, giving an effective semileptonic decay mode ($t \to b\ell^+\nu$) and a hadronic decay mode ($t \to bjj$) of the LLP. Similarly, LLP decays to four or more final states are typically covered by the above inclusive definitions of decay modes; this provides motivation not to over-optimize experimental searches to the specific, exclusive features of a particular decay mode.

While it would be ideal to have separate experimental searches for each of the above decay modes (when distinguishable), it is rare for specific models to allow the LLP to decay in only one manner; as in the example of an LLP decaying to a top quark, a number of decay modes typically occur with specific predictions for the branching fractions. As another example, if the LLP couples to the SM via mixing with the SM Higgs boson, then the LLP decays via mass-proportional couplings giving rise to b- and τ-rich signatures. If, instead, the LLP decays through a kinetic mixing as in the case of dark photons or Z bosons, then the LLP can decay to any particle charged under the weak interactions, giving rise to a relatively large leptonic branching fraction in addition to hadronic decay modes. This allows some level of prioritization of decay modes based on motivated UV-complete models; for example, the Higgs-portal model prioritizes searches for heavy-flavor quarks and leptons in LLP decay, while the gauge-portal model prioritizes searches for electrons and muons in LLP decay. Ultimately, however, it is desirable to retain independent sensitivity to each individual decay mode as much as possible. Indeed, for each decay mode listed above, models exist for which the given decay mode would be the main discovery channel.

Invisible Final-State Particles: where invisible particles appear as products of LLP decays, additional model dependence arises from the unknown mass of the invisible particle. The invisible particle could be a SM neutrino, DM, an LSP in SUSY, or another BSM particle. The phenomenology depends strongly on the mass splitting, $\Delta \equiv M_{\text{LLP}} - M_{\text{invisible}}$. If $\Delta \ll M_{\text{LLP}}$ (*i.e.*, $M_{\text{LLP}} \sim M_{\text{invisible}}$), the spectrum is compressed and the visible decay products of the LLP are soft. This could, for instance, lead to signatures such as disappearing tracks or necessitate the use of ISR jets to trigger on the LLP signature. If the mass splitting is large, $M_{\text{invisible}} \ll M_{\text{LLP}}$, then the signatures lose their dependence on the invisible particle mass.

We suggest three possible benchmarks: a compressed spectrum with $\Delta \ll M_{\text{LLP}}$ (example: a nearly degenerate chargino-neutralino

pair, giving rise to soft leptons or disappearing tracks [56–58, 92, 121–123, 187, 188]); a massless invisible state, $\Delta = M_{\text{LLP}}$ (example: a next-to-lightest SUSY particle (NLSP) decaying to SM particles and a massless gravitino in gauge-mediated SUSY breaking [105, 194–199]); and an intermediate splitting corresponding to a democratic mass hierarchy, $\Delta \approx M_{\text{LLP}}/2$ (example: NLSPs in mini-split SUSY [54, 55, 89]).

2.4 *A Simplified Model Proposal*

In this section, we present a compact set of simplified model channels that, broadly speaking, covers the space of theoretical models in order to motivate new experimental searches. Such a minimal, compact set may not be optimal for reinterpretation of results (where variations on our listed production and decay modes may influence signal efficiencies and cross section sensitivities), but rather provides a convenient characterization of possible signals to ensure that no major discovery mode is missed. These models may therefore serve as a starting point for systematically understanding experimental coverage of LLP signatures and devising new searches, but may need to be extended in future for the purposes of facilitating reinterpretation. We undertake an in-depth discussion of these topics in Section 6.

We classify LLPs according to their SM gauge charges, as these dictate the dominant or allowed LLP production and decay modes, and can give rise to different signatures (for example, disappearing tracks and hadronized LLPs). We separately consider LLPs that are: (a) neutral; (b) electrically charged but color neutral; and (c) color charged. In the latter case, it is important to distinguish between the long-lived parton (which carries a charge under quantum chromodynamics, QCD) that hadronizes prior to decay, and the physical LLP, which is a color-singlet "R-hadron" (using the standard nomenclature inspired by SUSY). The decays of the R-hadron are still dominated by the parton-level processes.

All of the following models have the LLP mass and lifetime as free parameters. For heavy-parent (HP) production, the parent mass is an additional parameter, while for invisible decays, several different benchmarks for mass splittings between LLP and invisible final state may have to be separately considered as described in Section 2.3.2. The cross section may have a theoretically well-motivated target value depending on UV-model parameters, but phenomenologically can generally be taken as a free parameter.

We emphasize that in spite of the many simplified model channels proposed below, a small number of experimental LLP searches can have excellent coverage over a wide range of channels (at least for certain lifetime ranges). The list is intended to be comprehensive in order to identify whether there are new searches that could have a similarly high impact on the space of simplified models, and identify where the gaps in coverage are.

2.4.1 *Neutral LLPs*

The simplified model channels for neutral LLPs are shown in Table 2.1, where X indicates the LLP.

In our initial proposal, which is the first iteration of the simplified model framework, it is sufficient to consider as "jets" all of the following: $j = u, d, s, c, b, g$. It is worth commenting that b-quarks pose unique challenges and opportunities. Since b-quarks are themselves LLPs, they appear with an additional displacement relative to the LLP decay location. They also often give rise to soft muons in their decays, which could in principle lead to additional trigger or selection possibilities. However, these subtleties can be addressed in further refinements of the simplified models; we discuss this further in Section 2.6. Similarly, we consider e, μ, and τ to be included in the broad category of "leptons", with the proviso that searches should be designed where possible with sensitivity to each.

When multiple production modes are specified in one row of the table, this means that multiple especially well-motivated production channels give rise to similar signatures. Typically only one of these simplified model production modes will actually need to be included when developing and assessing sensitivity of an experimental search, but we sometimes include multiple different production modes as individuals may variously prefer one over the other.

In each entry of the table, we indicate which umbrella category of well-motivated UV models (Section 2.2) can predict a particular (production) $\times$ (decay) mode. An asterisk (*) on the umbrella model indicates that $\not{E}_{\mathrm{T}}$ is required in the decay. A dagger (†) indicates that this particle production $\times$ decay scenario is not present in the *simplest and most minimal* implementations or spectra of the umbrella model, but could be present in extensions of the minimal models. While the HIG production signatures are best-motivated for the SM-like 125 GeV Higgs, exotic Higgses of other masses can still have the same production modes and so m_H can be taken as a free parameter.

We remind the reader that the production modes listed in Table 2.1 encompass also the associated production of characteristic prompt objects. For example, the Higgs production modes not only proceed through gluon fusion, but also through VBF and VH production, each of which results in associated prompt objects such as forward jets in VBF, and leptons or $\not{E}_{\mathrm{T}}$ in VH. All of the production modes listed in Table 2.1 could be accompanied by ISR jets that aid in triggering or identifying signal events. It is therefore important that searches are designed to exploit such prompt AOs whenever they can improve signal sensitivity, especially with regard to triggering.

To demonstrate how to map full models onto the list of simplified models (and vice-versa), we consider a few concrete cases. For instance, if we consider a model of neutral naturalness where X is

Production \ Decay	$\gamma\gamma(+\text{inv.})$	$\gamma + \text{inv.}$	$jj(+\text{inv.})$	$jj\ell$	$\ell^+\ell^-(+\text{inv.})$	$\ell_\alpha^+\ell_{\beta\neq\alpha}^-(+\text{inv.})$
DPP: sneutrino pair or neutralino pair	†	SUSY	SUSY	SUSY	SUSY	SUSY
HP: squark pair, $\tilde{q} \to jX$ or gluino pair $\tilde{g} \to jjX$	†	SUSY	SUSY	SUSY	SUSY	SUSY
HP: slepton pair, $\tilde{\ell} \to \ell X$ or chargino pair, $\tilde{\chi} \to WX$	†	SUSY	SUSY	SUSY	SUSY	SUSY
HIG: $h \to XX$ or $\to XX + \text{inv.}$	Higgs, DM*	†	Higgs, DM*	RHν	Higgs, DM* RHν*	RHν*
HIG: $h \to X + \text{inv.}$	DM*, RHν	†	DM*	RHν	DM*	†
RES: $Z(Z') \to XX$ or $\to XX + \text{inv.}$	Z', DM*	†	Z', DM*	RHν	Z', DM*	†
RES: $Z(Z') \to X + \text{inv.}$	DM	†	DM	RHν	DM	†
CC: $W(W') \to \ell X$	†	†	RHν*	RHν	RHν*	RHν*

Table 2.1: **Simplified model channels for neutral LLPs.** The LLP is indicated by X. Each row shows a separate production mode and each column shows a separate possible decay mode, and therefore every cell in the table corresponds to a different simplified model channel of (production)×(decay). We have cross-referenced the UV models from Section 2.2 with cells in the table to show how the most common signatures of complete models populate the simplified model space. The asterisk (*) shows that the model definitively predicts missing energy in the LLP decay. A dagger (†) indicates that this particle production × decay scenario is not present in the *simplest and most minimal* implementations or spectra of the umbrella model, but could be present in extensions of the minimal models. When two production modes are provided (with an "or"), either simplified model can be used to simulate the same simplified model channel.

a long-lived scalar that decays via Higgs mixing (for instance, X could be the lightest quasi-stable glueball), then the process where the SM Higgs h decays via $h \to XX$, $X \to b\bar{b}$ would be covered with the HIG production mechanism and a di-jet decay. Entirely unrelated models, such as the case where X is a bino-like neutralino with RPV decays $h \to XX$, $X \to jjj$ could be covered with the same simplified model because most hadronic LLP searches do not have exclusive requirements on jet multiplicity. Similarly, a hidden-sector model with a dark photon, A', produced in $h \to A'A'$, $A' \to f\bar{f}$ would also give rise to the di-jet signature when f is a quark, whereas it would populate the $\ell^+\ell^-$ column if f is a lepton. Finally, a scenario with multiple hidden-sector states X_1 and X_2, in which X_2 is an LLP and X_1 is a stable, invisible particle, could give rise to signatures like $h \to X_2X_2$, $X_2 \to X_1jj$ that would be covered by the same HIG production, hadronic-decay simplified model; however, we see how $\not{E}_T$ can easily appear in the final state, and

that the LLP decay products may not be entirely hadronic. Therefore, the simplified models in Table 2.1 can cover an incredibly broad range of signatures, but only if searches are not overly optimized to particular features such as $\not{E}_{\mathrm{T}}$ and LLPs decaying entirely visibly (which would allow reconstruction of the LLP mass) [8].

[8] This should not, of course, be interpreted as saying that searches shouldn't be done that exploit these features. Instead, our position is that experiments should bear in mind the range of topologies and models covered by each cell in Table 2.1 when designing searches, and that some more inclusive signal regions should be established where possible.

2.4.2 *Electrically Charged LLPs:* $|Q| = 1$

For an electrically charged LLP, we need to consider far fewer production modes because of the irreducible gauge production associated with the electric charge. We still consider the additional possibility of a HP scenario where the parent has a QCD charge, as this could potentially dominate the production cross section, see *e.g.*, Ref. [88]. We summarize our proposals in Table 2.2.

Note that we group all resonant production into the Z' simplified model. The reason is that the SM Higgs cannot decay into two on-shell charged particles due to the model-independent limits from LEP on charged particle masses, $M \gtrsim 75-90$ GeV (see, for example, Ref. [200]); because of this lower limit on the LLP mass, it is less important to use AOs for triggering and reconstructing charged LLP signatures than for neutral LLPs. Additionally, there are fewer allowed decay modes because of the requirement of charge conservation.

For concreteness, we recommend using $|Q| = 1$ as a benchmark for charged LLPs for the purpose of determining allowed decay modes. Although other values of Q are possible, these often result in cosmologically stable charged relics or necessitate different decay modes than those listed here. Additionally, LLPs with $|Q| = 1$ are motivated within SUSY [56–58, 201–203] and within Type-III seesaw models of neutrino masses [204–207]. We note that there exist already dedicated searches for heavy quasi-stable charged particles with non-standard charges [208, 209]. Because such searches are by construction not intended to be sensitive to the decays of the LLP, the existing models are sufficient for characterizing these signatures and they do not need to be additionally included in our framework.

For massive particles with $|Q| = 1$ with intermediate or large lifetimes such that the LLP traverses a significant part (or all) of the tracker, the highly ionizing track of the LLP provides a prominent signature. This can be exploited for an efficient suppression of backgrounds while keeping identification and/or reconstruction criteria as loose and, hence, as inclusive as possible. In particular, for decay-lengths of the order of or larger than the detector size, the signature of highly ionizing tracks and anomalous time of flight (*i.e.*, searches for heavy stable charged particles; see Sections 3.5 and 6.4.1) constitute an important search strategy covering a large range of lifetimes present in the parameter space of theoretically motivated models. While the searches for heavy stable charged particles are largely inclusive with respect to additional objects in the event, they depend strongly on the velocity of the LLP. For $\beta \rightarrow$

Production \ Decay	ℓ + inv.	jj(+inv.)	$jj\ell$	$\ell\gamma$
DPP: chargino pair or slepton pair	SUSY DM*	SUSY DM*	SUSY	†
HP: $\tilde{q} \to jX$	SUSY DM*	SUSY DM*	SUSY	†
RES: $Z' \to XX$	Z′, DM*	Z′, DM*	Z′	†
CC: $W' \to X$ + inv.	DM*	DM*	RHν	†

Table 2.2: **Simplified model channels for electrically charged LLPs** such that $|Q| = 1$. The LLP is indicated by X. Each row shows a separate production mode and each column shows a separate possible decay mode, and therefore every cell in the table corresponds to a different simplified model channel of (production)×(decay). We have cross-referenced the UV models from Section 2.2 with cells in the table to show how the most common signatures of complete models populate the simplified model space. The asterisk (*) shows that the model definitively predicts missing energy in the LLP decay. A dagger (†) indicates that this particle production × decay scenario is not present in the *simplest and most minimal* implementations or spectra of the umbrella model, but could be present in extensions of the minimal models. When two production modes are provided (with an "or"), both production simplified models can be used to cover the same experimental signatures.

1 one loses the discriminating power against minimally ionizing particles, while for small velocities, $\beta \lesssim 0.5$, the reconstruction becomes increasingly difficult due to timing issues. It is therefore important to include the heavy parent production scenario which covers a much larger kinematic range than direct production alone and which may feature a much wider range of signal efficiencies than the DPP scenario [90].

While the signatures in Table 2.2 form a minimal set, they also encompass some scenarios that merit special comment. One of these is the disappearing track signature [56–58, 92, 121–123, 187, 188], in which a charged LLP decays to a nearly degenerate neutral particle. The lifetime is long in this scenario due to the tiny mass splitting between the two states. Formally, these are included in the chargino or slepton DPP modes in Table 2.2 with decays to ℓ + inv. or $q\bar{q}'$ + inv. taken in the limit where the splitting between the charged LLP and the invisible final state is of $\mathcal{O}(200\ \text{MeV})$. In the case of a hadronic decay, X decays to a soft pion that is very challenging to reconstruct and so the track simply disappears. This is an important scenario that is already the topic of existing searches [210, 211]. As the degeneracy between the charged LLP and the neutral state is relaxed, other signatures are possible; this parameter range is well motivated both by SUSY and DM models with coannihilation [91, 129, 130].

Production \ Decay	$j + \text{inv.}$	$jj(+\text{inv.})$	$j\ell$	$j\gamma$
DPP: squark pair or gluino pair	SUSY	SUSY	SUSY	†

Table 2.3: **Simplified model channels for LLPs with color charge.** The LLP is indicated by X. Each row shows a separate production mode and each column shows a separate possible decay mode, and therefore every cell in the table corresponds to a different simplified model channel of (production)×(decay). We have cross-referenced the UV models from Section 2.2 with cells in the table to show how the most common signatures of complete models populate the simplified model space. A dagger (†) indicates that this particle production × decay scenario is not present in the *simplest and most minimal* implementations or spectra of the umbrella model, but could be present in extensions of the minimal models. When two production modes are provided (with an "or"), both production simplified models can be used to cover the same experimental signatures.

Finally, we comment on the challenges of simulating the charged LLP simplified models. Because the LLP bends and interacts with detector material prior to its decay, the simulation of the LLP propagation is important in correctly modeling the experimental signature. The subsequent decay of the LLP must either be hard-coded into the detector simulation, or allow for an interface with programs such as Pythia 8 to implement the decays. We discuss the challenges of simulating signals for LLPs with electric or color charge in Section 2.5.2.

2.4.3 *LLPs with Color Charge*

An LLP charged under QCD is more constrained than even electrically charged LLPs. Because of the non-Abelian nature of the strong interactions, the gauge pair-production cross section of the LLP is specified by the LLP mass and its representation under the color group, $\text{SU}(3)_C$. We do not consider LLP production via a heavy parent particle because that cross section is unlikely to dominate the total production rate at the LHC relative to DPP. The simplified model channels are provided in Table 2.3.

A complication of the QCD-charged LLP is that the LLP hadronizes prior to its decay, forming an R-hadron bound state. The modeling of hadronization and subsequent propagation is directly related to many properties of the long-lived parton, such as electric charge, flavor, and spin. Event generators such as Pythia 8 have routines [212, 213] to simulate LLP hadronization, although it is unclear how precise these predictions are. For a point of comparison, using the default settings of Pythia 8 yields an estimate of the

neutral R-hadron fraction from a gluino (color-octet fermion, $\tilde{g}$) of approximately 54%, while the neutral R-hadron fraction for a stop (scalar top partner) is estimated to be 44% [89]. After hadronization, the charge of the R-hadron may change as it passes through the detector. For instance, some estimates [214, 215] suggest that heavy, color-octet gluinos $\tilde{g}$ would predominantly form mesons (*e.g.*, $(u\tilde{g}\bar{d})$) at first. They eventually drop to the lower-energy neutral singlet baryon $\tilde{\Lambda} = (\tilde{g}uds)$ state when interacting with the protons and neutrons within the calorimeters.

The modeling of LLP hadronization and propagation is crucial to designing searches for color-charged LLPs and assessing their sensitivity. For example, only the charged R-hadrons can be found in heavy stable charged particle search; if the LLP charge changes as it passes through the detector, heavy stable charged particle searches may have limited sensitivity. To take this into account, the experimental searches include both tracker-only or tracker+calorimeter signal regions [4, 216], which enhances sensitivity to the scenario in which R-hadrons lose their charge by the time they reach the calorimeters.

Because no R-hadrons have been discovered to date and hence their properties cannot be directly measured, R-hadron modeling in detector simulations is challenging. We discuss the challenges of simulating the propagation and decays of LLPs with color charge in Section 2.5.2.

2.5 *Proposal for a Simplified Model Library*

The simplified models outlined in the above sections provide a common language for theorists and experimentalists to study the sensitivity of existing searches, propose new search ideas, and interpret results in terms of UV models. Each of these activities demands a simple framework for the simulation of signal events that can be used to evaluate signal efficiencies of different search strategies and map these back onto model parameters. Requiring individual users to create their own MC models for each simplified model is impractical, redundant, and invites the introduction of errors into the analysis process.

In this section, we propose and provide a draft version of a *simplified model library* consisting of model files and MC generator cards that can be used to generate events for various simplified models in a straightforward fashion. Because each experiment uses slightly different MC generators and settings, this allows each collaboration (as well as theorists) to generate events for each simplified model based on the provided files. Depending on how the LLP program expands and develops over the next few years, it may become expedient to expand the simplified model library to include sets of events in a standard format (such as the Les Houches format [217]) that can be directly fed into event-generator and detector-simulation programs. Given the factorization of produc-

tion and decay of LLPs that is valid for neutral LLPs, this could involve two mini-libraries: a set of production events for LLPs and a set of decay events for LLPs, along with a protocol for "stitching" the events together.

The current version of the library is available at the LHC LLP Community website [9], hosted at CERN. In Appendix A, we also provide tables that list how to simulate each LLP simplified model channel with one of the specified base models. These proposals are based on the models outlined in Section 2.5.1 and often match the best-motivated simplified models from Section 2.4, and also building on the DM-inspired LLP simplified models proposed and detailed in Ref. [93]. The library currently focuses on models of neutral LLPs; simulating the propagation of charged LLPs along with the full range of decays listed in Sections 2.4.2–2.4.3 requires more careful collaboration with detector simulation and other MC programs to ensure that they can practically be used in experimental studies.

[9] http://cern.ch/longlivedparticles

We provide model files in the popular Universal Feynrules Output (UFO) format [218], which is designed to interface easily with parton-level simulation programs such as MadGraph5_aMC@NLO [219]. The goal is to cover as many of the simplified models of Section 2.4 with as few UFO models as possible; this limits the amount of upkeep needed to maintain the library and develops familiarity with the few UFO models needed to simulate the LLP simplified models. We provide specific instructions for how to simulate each simplified LLP channel along with the UFO models.

2.5.1 *Base Models for Library*

In order to reproduce the simplified model channels of Section 2.3, we need a collection of models that:

- Includes additional gauge bosons and scalars to allow vector- and scalar-portal production of LLPs (RES and HIG);
- Includes new gauge-charged fermions and scalars to cover direct and simple cascade production modes of LLPs (DPP and HP);
- Includes a RHN-like state with couplings to SM neutrinos and leptons (CC);
- *Recommended, but optional:* allows for the decays of the LLP particle through all of the decay modes listed in Section 2.3, either through renormalizable or higher-dimensional couplings. If couplings that allow LLP decay are included in the UFO model, then the decays can be performed directly at the matrix-element level in programs such as MadGraph5_aMC@NLO [219] and accompanying packages such as MadSpin [220]. Alternatively, it is possible for neutral LLPs to simulate the production and decay as a single process; in such cases, numerical instabilities sometimes arise, for which dedicated event generators are

needed [48]. If the couplings needed for LLP are not in the UFO model, then LLPs can be left stable at the matrix-element level and decays implemented via Pythia 8 [212, 213], which allows for the straightforward implementation of decays according to a phase-space model, but does not correctly model the angular distribution of decay products. Instructions for implementing decays in Pythia are included with the model library files.

Fortunately, an extensive set of UFO models is already available for simulating the production of BSM particles. We note that extensions or generalizations of only three already-available UFO models are needed at the present time; the SUSY models in particular can cover many of the simplified models since they contain an enormous collection of new fermions and scalars. We also provide an optional fourth model, the Hidden Abelian Higgs Model, that can be helpful to simulate HIG and ZP theories.

1. **The Minimally Supersymmetric SM (MSSM):** the use of this model is motivated by and allows for the simulation of SUSY-like theories. The model contains a whole host of new particles with various gauge charges and spins. Therefore, an MSSM-based model allows for the simulation of many of the simplified model channels. In particular, we note that existing UFO variants of the MSSM that include gauge-mediated supersymmetry breaking (GMSB) couplings (including decays to light gravitinos), R-parity violation (making unstable the otherwise stable LSPs [52, 103, 104]), and the phenomenological MSSM (pMSSM) [221, 222] already cover most of the SUSY-motivated LLP scenarios. In some cases, the model is modified to give direct couplings between the Higgs states and gluons/photons.

2. **The Left−Right Symmetric Model (LRSM):** this UFO model is best for simulating UV theories with right-handed neutrinos (RHν). The UFO model supplements the SM by an additional $\mathrm{SU}(2)_\mathrm{R}$ symmetry, which gives additional charged and neutral gauge bosons. The model is available in the simplified models library and contains a right-handed neutrino which is the typical LLP candidate. The LLP can be produced via SM W, Z, or via the new gauge and Higgs bosons (both charged and neutral) present in the theory [10]. The LRSM therefore contains many of the charged and neutral current LLP production processes outlined in Section 2.4.1.

3. **Dark-Matter Simplified Models (DMSM)**: these UFO models are best for simulating UV theories in the DM class. These UFO models have been created by the LHC DM working group [79]. They typically consist of a new BSM mediator particle (such as a scalar of a Z') coupled to invisible DM particles. The UFO models can either be modified to include an unstable LLP, or else the otherwise stable "DM" particle can be decayed via Pythia. The utility and applicability of the DM simplified model framework

[10] Additional LRSM tools are available at https://sites.google.com/site/leftrighthep/.

to LLPs has already been demonstrated with a detailed proposal and study of classes of DM simplified models for LLPs [93]. These models are particularly good for simulating LLP production via a heavy resonance (RES), and can also simulate continuum production of LLPs in the limit where the mediator is taken to be light and off-shell (DPP).

4. **(optional) The Hidden Abelian Higgs Model (HAHM):** this UFO model contains new scalars and gauge bosons and so can be used to simulate both Higgs-portal and gauge-portal (ZP) theories. The model consists of the SM supplemented by a "hidden sector" consisting of a new U(1) gauge boson and a corresponding Higgs field. The physical gauge and Higgs bosons couple to the SM via kinetic and mass mixing, respectively. The HAHM allows for straightforward simulation of Higgs-portal production of LLPs, as well as Z' models and many hidden sector scenarios. The UFO implementation is from Ref. [223].

If additional decay modes are needed beyond those in the specified simplified models, then the library can be updated to include the new couplings mediating the decay. Alternatively, the LLPs can be left stable at parton level and decayed in event generators such as Pythia.

A detailed list of processes that can be used to simulate each simplified model channel is provided in Appendix A. The primary purpose of the library is to be used to simulate events for determining acceptances, and, as a result, the signal cross section is not important. Thus, for example, SM gauge interactions can be used as proxies for much weaker exotic interactions. Similarly, the spins of the particles are generally of subdominant importance: replacing the direct production of a fermion with the direct production of a scalar will not fundamentally alter the signature. As long as results are expressed in terms of sensitivity to cross sections and not couplings, the results can be qualitatively (and in many cases, quantitatively) applied to any similar production mode regardless of spin. However, we caution the reader that changing the spin of the LLP (or its parent) can change the angular distribution, and since in some cases LLP searches are typically more sensitive to aspects of event geometry than prompt searches, the second-order effects of spin could have more of an effect than for prompt simplified models.

2.5.2 *LLP Propagation and Interaction with Detector Material*

Long-lived particles with electric or QCD charges interact with the detector material prior to decay, and their propagation through the detector must be correctly modeled. The propagation of both LLPs with color charge (in the form of R-hadrons) and electrically charged LLPs can be implemented in the Geant4 (G4) toolkit [224]. For example, routines exist to simulate the propagation of color-

charged LLPs [225, 226]. G4 also includes routines that can implement N-body decays of LLPs using a phase-space model. This works fine for decays of LLPs to leptons, photons, invisible particles such as neutrinos, as well as exclusive hadronic decays.

However, G4 cannot implement decays to partons that subsequently shower and hadronize. One solution to this limitation is employed by CMS [227, 228] and ATLAS [229] in their searches for stopped LLPs. In these analyses, the signal simulation proceeds in two stages. During the first stage, the production of the LLP and its subsequent interactions with the detector are simulated. Once the stopping point of the LLP is determined, a new event is simulated including the LLP decay; the LLP decay products are then manually moved to the stopping point from the first stage. G4 is then run a second time to determine the efficiency for reconstructing the LLP decay signal.

It would be preferable to fully automate the simulation of decays of charged LLPs after propagation in G4. There exists in G4 a class called G4ExtDecayer, which can be used to implement decays by interfacing with an external generator. This class has been used to interface G4 with Pythia 6 [11]. The interface with Pythia 6 has been used most recently to model LLP gluino propagation and decay in a search for displaced vertices and missing energy in ATLAS [230]. Work is ongoing to extend this functionality to Pythia 8 and to simplify the interface.

[11] See http://geant4-userdoc.web.cern.ch/geant4-userdoc/Doxygen/examples_doc/html/Exampledecayer6.html

An additional challenge of simulating LLP decays is that, if the LLP undergoes a multi-body decay, generators such as Pythia use a phase-space model to implement the decays. If more accuracy is required, it may be preferable to use the full matrix element via generators such as MadGraph5 [219, 231]. If the matrix element is important for computing the decay of the LLP, then either an interface with MadGraph is needed to implement the decay prior to passing the vertex back to Pythia 8 for showering and hadronization, or matrix-element-based methods within the event generator itself must be used.

Because of the need to interface with G4 in simulating the decays of LLPs with electric or color charges, we do not at this point include such decay modes in our simplified model library. The decays of such LLPs will be most easily simulated via an interface with Pythia 8 once it is finalized.

Finally, we comment that LLPs can have even stranger propagation properties than LLPs with electric or color charges. For example, quirks are LLPs that are charged under a hidden-sector gauge interaction that confines at macroscopic scales [175]. Because the confinement scale can be just about any distance, quirks can have very unusual properties; as a specific example, if electrically charged quirk-antiquirk pairs are bound on the millimeter or centimeter level, they behave as an electric dipole and therefore do not leave conventional tracks that bend in the magnetic field. Other confinement scales give rise to different behaviors, such as meta-

stable heavy charged particles and non-helical tracks [232, 233]. In scenarios where the quirks carry color charge, the quirks hadronize and can undergo charge-flipping interactions as they move through the detector. These quirk scenarios can be challenging to model, and no public code exists that allows for the propagation and interaction of quirks with the detector material; we encourage the collaborations to validate and release any internal software they may have to study the propagation of quirks (for more discussion, see the discussion of quirks in Section 3.5) [12].

[12] Ideally, this software would be well-documented to facilitate sharing between experiments. A successful example of readily shareable software between experiments is the G4 package for *R*-hadrons and other particles' interaction with matter, found at http://r-hadrons.web.cern.ch/r-hadrons/

2.6 *Limitations of Simplified Models & Future Opportunities*

We conclude our discussion of simplified models with a more extensive discussion of the limitations of the current simplified model proposal in its application to models of various types, along with opportunities for future development. The presented framework is only the first step of a simplified model program that is comprehensive in terms of generating LHC signatures and allowing straightforward reinterpretation of experimental results for UV models. The framework we have developed with separate, modular components for LLP production and decay is amenable to expansion, and we encourage members of the theory and experimental communities to continue to do so over the coming years to ensure maximal utility of the simplified models framework.

One significant simplification we have undertaken in our framework is to define a "jet" as any of $j = u, c, d, s, b, g$. In reality, different partons give rise to different signatures, especially when one of the "jets" is a heavy-flavor quark. Jets initiated by b and c quarks have some useful distinguishing features, such as the fact that the underlying heavy-flavor meson decays at a distance slightly displaced from the proton interaction vertex and that there are often associated soft leptons resulting from meson decays. In particular, it is possible that the soft muons associated with B-meson decays could be used to enhance trigger and reconstruction prospects for LLPs decaying to b-jets [234]. However, heavy quarks also constitute an important backgrounds for LLP searches, and so LLPs decaying to b- and c-jets may necessitate dedicated treatment in future. Similarly, LLP decays to τ leptons may merit further specialized studies.

Another property of the current framework is that it is restricted to LLP signatures of low multiplicity. By "low multiplicity", we mean collider signatures with one or two LLPs. Searches inspired by these models are also suitable for many scenarios with three or four LLPs per event (which include models with dark-Higgs decays into lepton-jets [148], or left−right symmetric models [162]), since the LLP signatures are generally extremely rare and so only one or two typically need to be identified in a given event to greatly suppress backgrounds. Thus, as long as the search is inclusive with respect to possible additional displaced objects, the signature can

be covered with low-multiplicity strategies. As the LLP multiplicity grows, however, the simplified model space we have presented requires modification. This is both because the individual LLPs grow softer, making them harder to reconstruct on an individual level, and they become less separated in the detector, which makes isolation and identification of signal a challenge. On the other hand, the high LLP multiplicity may allow for new handles for further rejecting backgrounds, and the kinematics can vary widely based on the model (for example, in some "quirky" scenarios, LLPs can be produced in a variety of ways with different kinematic distributions [113]). In extreme cases, signals can even mimic pile-up [235]. High-multiplicity signatures therefore require dedicated modeling, and we defer the study of these signatures to Chapter 7.

Finally, we conclude by noting that simplified models are intended to provide a general framework to cover a broad swath of models. Any simplified model set-up, however, cannot cover every single UV model without becoming as complex as the UV model space itself. As with the case of promptly decaying new particles, care must also be taken in the interpretation of simplified models [71, 79–81, 99]: for example, constraints on simplified models assuming 100% branching fractions of LLPs to a particular final state may not accurately represent the constraint on a full model due to the large multiplicity of possible decay modes. There will additionally always be very well-motivated models that predict specific signatures that are challenging to incorporate into the simplified model framework outlined here. Experimental searches for these signatures should still be done where possible, but we encourage theorists and experimentalists alike to think carefully about how to design such searches so as to retain maximal sensitivity to simplified models that may give rise to similar signatures.

3
Experimental Coverage of Long-Lived Particle Signatures

Contents

Chapter editors: Juliette Alimena, Xabier Cid Vidal, Albert de Roeck, Jared Evans, Heather Russell, Jose Zurita

Contributors: David Curtin, Alberto Escalante del Valle, Philippe Mermod, Antonio Policicchio, Brian Shuve

A critical component of any discussion of long-lived particle searches at the LHC is the comprehensive review of the existing searches from ATLAS, CMS, and LHCb, and an assessment of their coverage and any gaps therein. This is an inherently challenging task, given the varied and atypical objects often defined and utilized in LLP analyses and the differences among the experiments. As such, the following discussion assumes little-to-no background on LLP search strategies and includes a high level of detail regarding the current analyses. The focus of the discussion is on the existing studies, while acknowledging that the landscape for new physics models and LLP signatures can be broader than the ones described here.

Backgrounds to most of these studies are typically small, as most LLP signatures are not naturally mimicked by any irreducible SM processeses. Backgrounds for LLP searches typically include peripheral or machine effects, those rarely important for searches for prompt physics, including cosmic muons, beam halo, detector noise, and cavern backgrounds. Such backgrounds are discussed in detail in Chapter 4. As rare as these backgrounds typically are, their rates are not completely negligible, and particular, model-dependent selection requirements (based on, for instance, the LLP mass range or specific decay modes) must be made to reduce backgrounds as much as possible and, in some cases, make the searches "background-free". Additionally, many default object reconstruction algorithms are not designed to detect particles originating from decays of LLPs, and so dedicated reconstruction of tracks, jets, leptons, or other objects may be required for LLP searches. Taken altogether, these factors make LLP searches very different from searches for prompt objects, and the following discussion additionally aims to collate and summarize the current techniques for LLP reconstruction at the LHC.

A particular challenge for many LLP signatures is the trigger. With the exception of certain dedicated ATLAS triggers in the calorimeters or muon spectrometer, there are no Level-1 (L1) triggers that directly exploit the displaced nature of LLP decays, and L1 trigger thresholds must be surpassed by standard objects (such as leptons or high-energy jets) for the event to be recorded. [1] Throughout this chapter, we highlight the role and limitations of the trigger(s) employed in current searches, and the design of customized LLP triggers is to be encouraged to probe new and otherwise inaccessible regions of parameter space.

[1] It is true that, depending on the signature, some of these caveats can be circumvented by a sensible use of existing prompt triggers. For example, photon triggers will collect displaced electrons, calorimeter/jet triggers will record displaced hadronic vertices, etc.

A detailed review of all existing searches is presented in Sections 3.1 through 3.5. This survey of the current experimental coverage aims to highlight the highest-priority searches still yet to be performed, which we summarize in Section 3.6. In all cases, we focus on the latest version of each analysis. Notably we will typically present searches based on data taken at a center-of-mass energy

$\sqrt{s} = 13$ TeV, and discuss searches using Run 1 data only when the newer version is not yet available, or when there are conceptual differences between two versions of the same analysis.

Because long-lived particles travel macroscopic distances in the detectors, many of the search strategies rely on the identification of displaced objects, namely SM particles (charged leptons, photons, hadrons, jets) that are produced at a location away from the primary vertex (PV) where the hard pp collision takes place. The secondary vertex at which the decay of the LLP occurs is referred to as a displaced vertex (DV). As far as possible, our classification of searches is linked to the parton-level objects produced in LLP decays, which allows a relatively straightforward linkage to LLP models (as well as simplified models; see Chapter 2). Borrowing the terminology from prompt searches, we consider the following categories for the analogous displaced objects produced in LLP decays: all-hadronic (jets), leptonic, semi-leptonic, and photonic. However, we caution the reader that these "jets" or "photons" may not be of the standard type, and so other objects may pass the selections of these analyses. The remaining searches fall in the "other long-lived exotics" category, mostly consisting of non-standard tracks (disappearing tracks, heavy stable charged particles, quirks, etc.), but also including some trackless signals, such as stopped particles and Strongly Interacting Massive Particles (SIMPs). These categories are not to be interpreted as exclusive; many models and searches could fit into several categories. [2] For example, Refs. [236–238] show how searches for different signatures and LLP lifetimes can be combined to cover large parts of the parameter spaces of particular UV models.

[2] Another important ingredient of the LLP searches is the possibility to reinterpret their results to a large variety of models, namely be able to *recast* them. While we refer the interested reader to Chapter 6 it is worth mentioning here that many existing searches publicly provide useful recasting information, such as efficiency maps or model-independent bounds on production cross sections.

3.1 *All-Hadronic Decays*

ATLAS has several searches for displaced decays with hadronic objects, including searches for two objects decaying in the hadronic calorimeter (HCAL) [239, 240]; decays within the muon system (MS) or inner detector (ID) [241]; ID decays in association with large $\not{E}_{\mathrm{T}}$ [230]; and ID decays in association with large $\not{E}_{\mathrm{T}}$, jets, or leptons [189]. CMS has inclusive searches for displaced jets using 13 (8) TeV data [242, 243] ([244]). Moreover, the CMS displaced jets searches are relatively inclusive and so also cover LLPs with semi-leptonic decays despite having no specific lepton requirements. CMS also has a search for displaced vertices in multijet events [245]. LHCb has searches for both one [246] and two [247] all-hadronic DVs in their detector. Here the discussion is restricted to summarizing the hadronic channels, while those studies including leptons [189, 242] will be revisited in Sections 3.2 and 3.3 for the fully-leptonic and semi-leptonic cases, respectively.

3.1.1 *ATLAS Searches*

The reconstruction of displaced tracks in the ATLAS ID [248] follows a two-step procedure. In the first iteration, the default track identification algorithm is applied, which uses hits in the pixel system, Semiconductor Tracker (SCT), and Transition Radiation Tracker (TRT) to reconstruct tracks with a small impact parameter. The hits not associated to a track during the first pass are used in a second run of the track finder, with loose requirements on the transverse and longitudinal impact parameters (d_0 and z_0) and the number of silicon hits that are shared (or not shared) with another track. This two-step procedure is referred to as the *large radius tracking* (LRT) algorithm by the ATLAS collaboration. Applying the LRT procedure is CPU-intensive, and thus it is only run once per data-processing campaign, on a subset of specially-requested events [248].

In searches where the LLPs decay exclusively in the ID, standard triggers are used to select events with high-p_T jets, $\not{E}_T$, or high-p_T leptons [189, 230]. An ATLAS 13 TeV search [230] uses a standard $\not{E}_T$ trigger and an offline requirement of $\not{E}_T > 250$ GeV. The 8 TeV search [189] covers a larger range of topologies, and the event must have either $\not{E}_T > 180$ GeV or contain four, five, or six jets with $p_T > 90$, 65, or 55 GeV to pass the trigger. In both searches, the ID vertex is required to have at least 5 tracks and the invariant mass of the displaced vertex tracks to fullfil $m_{DV} > 10$ GeV. These searches are interpreted in the context of various SUSY scenarios involving gluinos or squarks decaying into leptons, jets and missing energy, namely R-Parity-Violating (RPV), General Gauge Mediation (GGM), and split SUSY. In the latter case R-hadrons [3] are considered. The particular LLP decay topology determines which trigger and analysis mode (specified by jet and lepton multiplicity, small/large $\not{E}_T$, etc.) has the best sensitivity. The LLPs covered by these searches are typically high mass ($\gtrsim 100$ GeV), and correspond to the direct-pair-production and heavy-parent production modes with hadronic decays (in the language of the simplified models presented in Section 2). However, these searches do not have sensitivity to low-mass LLPs, especially those resulting from the Higgs, Z', or charged-current production portals and then decaying hadronically.

[3] R-hadrons form when BSM colored particles hadronize due to a lifetime larger than the hadronization scale. In split SUSY the R-hadrons are typically long-lived due to their decays being mediated by heavy squarks.

For LLPs decaying in the HCAL or MS, dedicated *CalRatio* and *MuonRoI* triggers are employed [239–241, 249], allowing the searches to place limited requirements on the non-displaced portion of the event. We describe these triggers in more detail shortly. The efficiency of these triggers is 50% – 70% for decays within the relevant geometric detector region, and negligible outside of them (see Figure 3 of Ref. [241]). The results of these analyses are interpreted in terms of a $\Phi \to ss$ model, where Φ is a heavy scalar boson with 100 GeV $< m_\Phi <$ 1000 GeV and s is a long-lived, neutral scalar decaying to hadrons with branching fractions dictated by the Yukawa coupling. This can map to Higgs or Z' production modes

and hadronic decay mode in the simplified models.

The CalRatio trigger selects events with at least one trackless jet that has a very low fraction of energy deposited in the ECAL [4]. These CalRatio jets are characteristic of an LLP that decays within or just before the HCAL. The 13 TeV analysis [239] requires two CalRatio jets, where the exact CalRatio criteria are determined using a series of machine learning techniques to optimally discriminate the displaced decay signature from QCD jets and beam-induced background. Using the simplified $\Phi \rightarrow ss$ model with 125 GeV $< m_\Phi <$ 1000 GeV and 5 GeV $< m_s <$ 400 GeV, good sensitivity is observed for $c\tau$ between 0.05 and 35 m, depending on the Φ and LLP masses. Notably, SM-like Higgs boson decays to LLP pairs are constrained below 10% branching ratio in the most sensitive lifetime ranges, with exact limits dependent on the LLP mass [239]. The 8 TeV result also requires two CalRatio jets, and shows sensitivity for 100 GeV $< m_\Phi <$ 900 GeV and 10 GeV $< m_s <$ 150 GeV [240]

The MuonRoI trigger selects events with clusters of L1 Regions of Interest (RoIs) in the MS that are isolated from activity in the ID and calorimeters. It is efficient for LLPs that decay between 3 – 7 m transversely or 5 – 13 m longitudinally from the PV, for LLP masses greater than 10 GeV. After trigger selection, the ATLAS analysis in question requires either two reconstructed DVs in the MS [250] or one ID vertex and one MS vertex [241]. This ID–MS combination provides increased sensitivity to shorter lifetimes than an analysis only considering MS vertices, and shows good sensitivity to 100 GeV $< m_\Phi <$ 900 GeV and 10 GeV $< m_s <$ 150 GeV. Decays of a SM-like Higgs boson to LLP pairs are constrained below 1% in the most sensitive $c\tau$ regions (with cross section limits as low as 50 fb). The efficiency degrades for benchmarks with higher LLP boosts or very low mass LLPs, as fewer tracks are reconstructed. Another ATLAS search includes signal regions with only 1 DV in the MS, with sensitivity to SM-like Higgs decays to LLPs extending down to branching fractions of 0.1% [251]; this search also presents constraints on a wide range of models that helps facilitate reinterpretation for other BSM scenarios. In addition, a combination of the results from this search with the results from the 13 TeV CalRatio search was performed in Ref. [239] for the models common to both, and provides a summary of the ATLAS results for pair-produced neutral LLPs.

Recently, ATLAS presented a new study for hadronically decaying LLPs produced in association with a leptonically decaying Z boson [252]. In this analysis, the LLP decays inside of the HCAL. The use of lepton triggers on the associated Z decay products gives sensitivity to production of a *single* low-mass LLP, whereas other searches typically require 2 DVs; it is therefore an excellent example of the utility of prompt associated objects in obtaining sensitivity to low-mass LLPs. The model constraints are expressed in terms of a Higgs portal model where the SM-like Higgs decays to a bosonic

[4] The variable used to discriminate between CalRatio jets and standard jets is $\log_{10}(E_{\text{HAD}}/E_{\text{EM}})$, where E_{HAD} and E_{EM} are the fractions of the measured energies of the jets appearing in the HCAL and ECAL, respectively. The trigger selects trackless jets with $\log_{10}(E_{\text{HAD}}/E_{\text{EM}}) > 1.2$, which corresponds to an electromagnetic fraction of 0.067.

LLP.

With the exceptions of Refs. [189, 230, 252], which require prompt activity in addition to the DV and have comparatively high trigger thresholds, the ATLAS all-hadronic analyses require two DVs, and thus are insensitive to models that produce a single DV inside the detector [5].

[5] This may be the result of a signal that produces two DVs, but the lifetime is sufficiently long that only one DV appears inside the detector.

3.1.2 *CMS Searches*

The CMS analyses [242–244] are based on a dedicated offline *displaced jet tagging* algorithm using tracker information to identify pairs of displaced jets. The triggers used here are based on large values of $H_T = \sum |p_{T,j}|$ = 350 (500) GeV for 8 (13) TeV, where the H_T sum runs over all jets with $p_{T,j} > 40$ GeV and $|\eta_j| < 3.0$. The trigger for the 13 TeV analysis based on 2015 data additionally requires either two jets with $p_T > 40$ GeV and no more than two associated prompt tracks ($d_0 < 1$ mm) and the H_T threshold is lowered to 350 GeV if the two jets each have at least one track that originates far from the PV [6]. Only events with two or more displaced jets are kept in the analysis, while those with only one are used as a control sample to estimate the prompt jet misidentification rate. For $c\tau <$ 3 mm [7], the algorithm is inefficient as more than two tracks tend to have impact parameters less than 1 mm; for $c\tau > 1$ m the search is inefficient as most decays occur too far from the PV to form reconstructable tracks. A key difference among these searches is that the 8 TeV [244] and 13 TeV (2016 data) [243] analyses explicitly reconstruct the DV, while the 13 TeV (2015 data) [242] analysis does not.

[6] In this case this is defined by requiring that the transverse impact parameter significance $|d_0|/\sigma_{d_0}$ have a value greater than 5.

[7] Note that in principle the low $c\tau$ regime can be covered with standard triggers, however they require higher H_T thresholds.

CMS interprets the signal in several benchmark models that can be mapped to the direct pair production simplified model production mode, including a neutral LLP decaying hadronically and a color-charged LLP decaying into a jet plus a lepton. For neutral LLP pair production decaying democratically into light jets, the trigger efficiencies for $c\tau = 30$ mm are reported to be 2, 41, 81, and 92% for 50, 100, 300, 1000 GeV masses, respectively. It is evident that the requirements on H_T and on $p_{T,j}$ make the search inefficient for low LLP masses. Indeed, a phenomenological recast of the 8 TeV analysis [244] in terms of rare decays of a SM-like Higgs boson with a mass of 125 GeV Higgs sets very mild bounds for LLP masses below $m_h/2$ [253]. Thus, the CMS search has limited sensitivity to low-mass, hadronically decaying LLPs through the Higgs, Z', or charged-current simplified production modes.

As mentioned above, CMS also has a search for displaced vertices in multijet events [245], which was released near the time of the final editing of this manuscript.

3.1.3 *LHCb Search*

The LHCb searches [246, 247] trigger directly on DVs with a transverse distance of $L_{xy} > 4$ mm) with four or more tracks, vetoing

dense material regions in which hadronic interactions with the detector can mimic LLP decays. The trigger thresholds are, however, low. For example, the invariant mass of particles associated with the vertex must exceed 2 GeV and the scalar sum p_T of tracks at the vertex must exceed 3 GeV. Jet reconstruction is then performed offline with standard algorithms. The benchmark model used by these searches is a scalar particle decaying to two neutral LLPs, π_v (dark or "valley" pions), which corresponds to the Higgs simplified model with hadronic decay modes. The parent particle can be either a SM-like 125 GeV Higgs [246] or a Higgs-like scalar with mass in the 80–140 GeV range [247]. The search is performed for π_v masses between 25 and 50 GeV and decay lenghts between 0.6 and 15 mm. It is expected that LHCb will extend their coverage to shorter lifetimes by improving the understanding of the material and to lower masses by using fat-jets and jet-substructure to access larger boosts [254]. In principle, the search is also sensitive to direct pair production of LLPs.

Because of the low thresholds, the LHCb search focuses on low-mass LLPs with short lifetimes, for which it has excellent sensitivity. However, its sensitivity for other signatures is limited by the geometry of the detector and the LHCb luminosity compared to ATLAS and CMS. A model-dependent direct comparison among the LHCb, ATLAS and CMS reaches for the Higgs production mode decaying into dark pion LLPs can be seen in Figure 3.1.

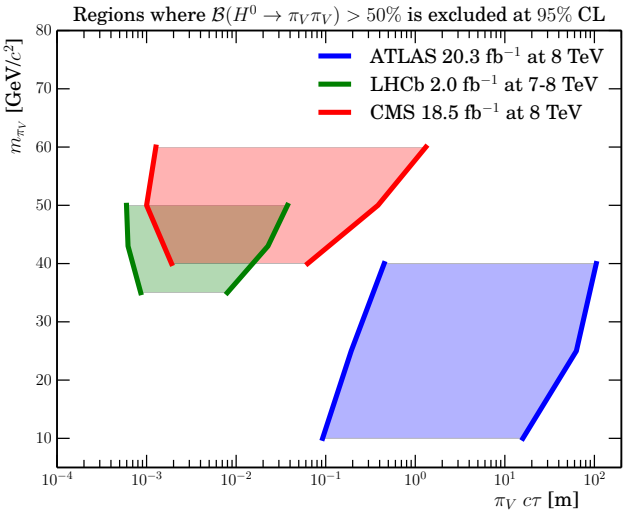

Figure 3.1: Comparison of the ATLAS [189], CMS [244] and LHCb [246] reaches for dark pions π_V decaying into jets. The CMS result is taken from the recast done in reference [253] of the 8 TeV analysis [244]. In the shaded regions $B(H \to \pi_v\pi_v)$ is constrained to be below 50%. Note that the ATLAS reach extends to higher masses as well; the plot was produced using the benchmark scenarios presented in [189], hence the meaningful bound is on the lifetimes. Taken from Ref. [246].

3.1.4 *Summary*

Searches in hadronic final states do not currently cover LLP parent masses below $\sim$ 100 GeV in a comprehensive way. This is typically due to the large $p_{T,j}$ requirements at the trigger level, with an exception being the DV reconstruction at LHCb. Additionally, the powerful ATLAS searches for LLPs decaying in the HCAL or MS require two LLP decays in the detector, meaning that as of this writing there is no sensitivity to singly produced long-lifetime LLPs with hadronic decays [8]. While the existing searches are typically sensitive to both direct pair production and heavy parent production of LLPs, not all of the searches provide benchmarks with a variety of LLP production kinematics and boost.

[8] Highly-inclusive searches for single LLPs decaying in the ATLAS MS have been proposed [255], finding that backgrounds are appreciable and need to be controlled using data-driven methods.

A potential way to extend the sensitivity of current analyses is to use other existing triggers exploiting such things as VBF production modes, leptons, $\not{E}_T$, etc., to trigger on associated *prompt* objects and perform the hadronic DV reconstruction offline. The ATLAS 8 TeV study [189] does employ multiple triggers (such as lepton triggers), but in each case the triggered object must be associated with the DV (for a lepton trigger, the lepton must originate from the DV). If, instead, a prompt lepton or VBF trigger were used with the offline reconstruction of a separate displaced object, sensitivity could be recovered to low-mass hadronic DVs in a variety of simplified models, including Higgs production (via VBF or VH associated production modes) [253, 256] or charged-current production (in association with a prompt lepton) [257]. In particular, triggering on associated prompt objects would improve the efficiency of reconstructing low-mass hadronic LLPs produced in the decays of a SM-like 125 GeV Higgs. As there is no theoretical lower limit on the masses of light neutral LLPs, it is imperative to lower the LLP mass coverage as much as possible. If at all possible, a dedicated *online* reconstruction of DVs would allow for a further reduction on the p_T threshold, giving sensitivity to light LLP masses.

3.2 *Leptonic Decays*

All three experiments have searches for a pair of leptons coming from a DV [189, 258–262]. CMS also has a search requiring exactly one isolated muon and one isolated electron (i.e., events with additional isolated leptons are discarded) with large transverse impact parameters (0.2 cm $< |d_0| <$ 10 cm), but without any other additional requirement including, for example, that the reconstructed tracks do not need to point to a common vertex [190]. This loose selection makes the search sensitive to a variety of new physics scenarios. Light and boosted LLPs can decay into collimated light leptons, dubbed *lepton-jets* [120], which are searched for at both CMS [263, 264] and ATLAS. ATLAS has searches for both displaced [265, 266] and prompt lepton-jets [267]. The LHCb collaboration also looks for light, neutral LLPs decaying into $\mu^+\mu^-$ pairs

by studying B-meson decays to kaons, for exclusive decay channels for both neutral [260] and charged [261] B-mesons, as well as dark photons that decay to muon pairs [262].

3.2.1 CMS Searches

The CMS searches trigger on leptons reconstructed using information from either the tracker [258] or the muon chambers [259], where the latter search uses only muons. In the tracker-based analysis, the LLP is reconstructed by forming pairs of charged leptons (where muons are required to have opposite signs), with p_T cuts of 26 GeV for muons, and 36 (21) GeV for the leading (subleading) electron. This yields slightly larger efficiencies in the muon channel. The transverse impact parameter $|d_0|$ needs to be 12 times larger than its uncertainty σ_d (approximately corresponding to a distance $\gtrsim$ 200 μm) to reject prompt backgrounds. In the MS-based analysis, muon candidates are reconstructed using hits in the muon chambers, and no information from the silicon tracker is used. In order to avoid biases from a loose beamspot constraint in the seeding step, these muons undergo an additional refit step. These candidates are referred to as *re-fitted stand-alone* (RSA) muons, and they need to fulfill $p_T > 26$ GeV, $|\eta| < 2$, and to be separated by $\Delta R > 0.2$. More importantly, these candidates are rejected if they can be matched to a $p_T > 10$ GeV track in the inner tracker, which efficiently excludes prompt muons and also renders this study fully complementary to the tracker-based one. Both these searches are interpreted in terms of decays of an SM-like Higgs H ($H \to XX, X \to l^+l^-$) and RPV squarks, covering proper lifetimes of 0.01–10^5 cm for the Higgs scenario, and 0.1–10^4 cm for the SUSY case. The difference in the lower reach of $c\tau$ is due to the larger boost factor of the Higgs. These benchmarks map to the direct pair production, heavy parent and Higgs production simplified models, with flavor-conserving leptonic decays of the LLP. There is good sensitivity down to relatively low masses (LLPs of masses $\gtrsim$ 20 GeV produced in Higgs decays) due to the low lepton trigger thresholds.

Additionally, CMS has a search for one electron and one muon, each with large transverse impact parameter (200 μm $< |d_0| <$ 10 cm) [190]. Events are selected using a dedicated trigger for $e\mu$ pairs that applies a p_T cut on the leptons (42 GeV for electrons, 40 GeV for muons) but, unlike standard triggers, places no restriction on the maximum d_0 or distance from the PV. Events with exactly one muon and exactly one electron are kept, and then separated into “prompt", “displaced control" and “signal" regions, defined as $|d_0| <$ 100 μm, 100 μm $< |d_0| <$ 200 μm, and $|d_0| >$ 200 μm, respectively. This selection makes the signal region almost free of leptons coming from SM processes, with rare tau-leptons, B-mesons or D-mesons as the largest remaining background.

Although in the original search the results are interpreted in

the context of long-lived RPV stops (excluding masses below 870 GeV for $c\tau = 2$ cm) [9], this search has been shown to be sensitive to many scenarios, including long-lived staus in gauge mediated SUSY breaking [198] and right-handed neutrinos [45]. Indeed, this search has sensitivity to LLPs produced via any of the simplified model production modes and (semi)-leptonic decays that give exactly one electron and one muon. On the other hand, models where long-lived particles decay only to *either* muons *or* electrons (*e.g.*, $\tilde{\mu} \to \mu\tilde{G}$) are unconstrained by this search. Furthermore, same-sign lepton signatures and signatures with additional leptons are not constrained by the current search but could be covered by extensions of the search [45, 198]. Due to the generality of tau-specific models, searches for hadronic tau channels is also desirable. This search has sensitivity to relatively low-mass LLPs; however, the 8 TeV analysis [268] has lower thresholds ($p_T > 22$ GeV on both leptons) albeit with a requirement for shorter decay distances ($|d_0| < 2$ cm), and so has superior sensitivity to very low-p_T displaced signals. Maintaining low trigger thresholds is necessary to obtain sensitivity to the lowest-mass leptonic LLP signals.

[9] We note that a CMS prompt search for leptoquarks has been recasted using the same model, finding stringent constraints for lifetimes below a few millimeters. This reinterpretation is discussed in detail in Section 6.7.

3.2.2 *ATLAS Searches*

The primary ATLAS search for displaced leptons [189] triggers on muons without an ID track, electrons, or photons [10]. The trigger and offline p_T criteria are relatively high, requiring one of the following: one muon of at least 50 GeV; one electron of at least 110 GeV; one photon of at least 130 GeV; or two electrons, photons, or an electron and a photon with minimum p_T requirements for both objects in the 38–48 GeV range. The DV is formed from opposite-sign leptons, irrespective of flavor, and needs to be located more than 4 mm away from the PV in the transverse plane. DVs in regions with dense detector material are vetoed to suppression backgrounds from converted photons (e.g., $\gamma p \to e^+e^- p$). This search is in principle sensitive to events with a reconstructed DV mass $m_{DV} > 10$ GeV, but the high p_T requirements for the leptons restrict the sensitivity to low-mass LLPs.

[10] Electrons with large transverse impact parameters d_0 tend to be missing a track at trigger level and are reconstructed as photons.

ATLAS has also recently released a search for pairs of muons that correspond to a displaced vertex [269]. This search is sensitive to LLP decays that occur sufficiently far from the interaction point that the muons are reconstructed only in the MS. The analysis has four separate trigger pathways: $\not{E}_T > 110$ GeV; one muon with $p_T > 60$ GeV and $|\eta| < 1.05$; two muons with $p_T \gtrsim 15$ GeV and $\Delta R_{\mu\mu} < 0.5$; or three muons with $p_T > 6$ GeV. Thus, the search has sensitivity to final states with high and low masses (down to $m_{\mu\mu} = 15$ GeV), as well as with various lepton multiplicities. Offline selections require the muons to have $p_T > 10$ GeV and opposite charge, and the search is efficient at reconstructing muons for transverse impact parameters up to $|d_0| = 200$ cm. Muons are also required to satisfy isolation requirements from jets as well as

from nearby tracks. The search puts constraints on a SUSY model and a model of dark photon production in Higgs decays; this can be used to determine sensitivity to all of the simplified production modes from Chapter 2 in the $\mu\mu$ decay mode (or $\mu\mu$ in association with other objects). It also demonstrates how combining many trigger pathways and loose selection requirements can enhance sensitivity to a wide range of LLP models.

3.2.3 *LHCb Searches*

LHCb has a search that looks for the direct production of both promptly decaying and long-lived dark photons [262]. As a result of the direct production, dark photons do not tend to be highly boosted in the transverse direction. Events [11] are required to have a single muon with $p_T > 1.8$ GeV, or two muons with a product of transverse momenta $\gtrsim (1.5\text{ GeV})^2$. The displaced search constrains previously uncovered dark photon parameter space around masses of ~ 300 MeV.

[11] For the prompt dark photon search, events are reconstructed at trigger level so that all online reconstructed particles are recorded, while the rest of event information is discarded [270]. The prompt search constrains entirely new territory above 10 GeV.

The LHCb searches for displaced leptons in rare B meson decays [260, 261] rely on standard techniques to identify the $B^{\pm}$ decay vertex and the kaons and pions in the event, and the dimuon invariant mass $m(\mu^+\mu^-)$ variable is scanned for excesses. The $X \to \mu^+\mu^-$ vertex is not required to be displaced from the $B^{\pm}$ vertex, and thus the constraints apply to both prompt and long-lived particles. The analysis probes LLP masses of 214 (250) MeV $< m_X <$ 4350 (4700) MeV for the $B^0 \to K^*\mu^+\mu^-$ ($B^+ \to K^+X, X \to \mu^+\mu^-$) process, with the mass range being limited by kinematics.

3.2.4 *Lepton-Jet Searches*

Searches for lepton-jets are focused on $\mathcal{O}(\text{GeV})$ LLP masses and distinctly boosted signatures, and thus we treat them separately.

The ATLAS 8 TeV search [265] considers three types of lepton-jets: those containing only muons, only electrons/pions, or a mixture of the two. The muon and electron/pion lepton-jets can contain either two or four leptons, while the mixed lepton-jet must contain two muons and a jet consistent with a displaced electron/pion pair. As these signatures contain relatively soft leptons, the ATLAS 8 TeV analysis uses a trigger that requires three muon tracks in the MS with $p_T > 6$ GeV. There is a built-in limitation to this trigger, which is that the L1 requirement of three separate muon RoIs makes it only sensitive to topologies with two lepton-jets in which one lepton-jet has a wide enough opening angle between two muons to create two level-one RoIs. For the electron lepton-jets, when the electrons are produced in the HCAL they are indistinguishable from a hadronic decay and thus the CalRatio trigger is used.

In the 13 TeV ATLAS analysis [266], a *narrow-scan* muon trigger is additionally used. This trigger starts off by selecting events with

one muon with $p_T > 20$ GeV, then requires a second muon with $p_T > 6$ GeV within $\Delta R = 0.5$ of the leading muon.

Both the 8 and 13 TeV ATLAS searches are interpreted for Higgs-like scalar particles (with masses of 125 and 800 GeV) that decay effectively into either two or four lepton pairs, with each lepton pair assumed to come from a low-mass "dark" photon, γ_D. The ATLAS result excludes exotic Higgs branching ratios below 10% for dark photon lifetimes $2 < c\tau < 100$ mm. Note that here γ_D is also allowed to decay to pions and so the results can also be interpreted for hadronically and semi-leptonically decaying LLPs. This corresponds to the Higgs production mode in the simplified models proposal with an admixture of flavor-conserving leptonic and hadronic LLP decays.

The CMS lepton-jet search focuses on fully muonic lepton-jets and has been performed with both the 8 TeV dataset [263] and part of the 13 TeV dataset [264]. The 13 TeV search is sensitive to di-muon parent particle masses up to 8.5 GeV. Events are selected with a di-muon trigger with standard isolation requirements. Further selection requires at least four muons, forming a minimum of two opposite-charged pairs. CMS uses a benchmark model with scalars decaying into either lighter scalars or dark photons, with varying scalar and dark photon mass. For the case of a 125 GeV Higgs they can exclude an exotic branching ratio of below 0.1% for some parameter points. The CMS search can be compared with the ATLAS results, as can be seen in Figure 3.2. We note that this study includes sensitivity to both prompt and displaced muonic lepton jets.

3.2.5 *Summary*

To summarize, the lepton searches rely on fairly standard lepton identification, with vertex reconstruction being performed mostly offline. Searches for leptonically decaying LLPs typically enjoy low trigger thresholds and good sensitivity to LLP production rates. Extending the success of the leptonic LLP program to future LHC running will necessitate maintaining low-threshold triggers for displaced leptons in a high-luminosity environment; this is a major challenge but one that must be overcome. Another outstanding challenge is coverage of LLP decays to τ leptons, which lie at the interface between hadronic and leptonic searches. Such decays are very well motivated from the theoretical point of view, as a Higgs-like scalar can typically decay about 300 times more often into $\tau^+\tau^-$ if kinematically allowed, and also one could have large rates into mixed decay modes such as $\tau^+\mu^-$. A displaced hadronic τ is a striking object, and most likely will have few backgrounds. Hence, limits on exclusive displaced τs would be of utmost importance [12].

As the leptonic searches explicitly require opposite-sign leptons, the same-sign lepton signature (motivated from Majorana neutrinos; see the LHCb search in Section 3.3, or heavy, doubly-charged

[12] We note that if the τ originates from outside the tracker, the hadronically decaying taus are indistinguishable from other displaced hadrons. For instance, in the ATLAS search utilizing muon RoIs [241] the results are interpreted for a model with a scalar particle with Higgs-like couplings to SM fermions, which includes a branching fraction into $\tau^+\tau^-$. However, if the τ originates from the ID, the low number of tracks associated to it (one to three) will not fulfill the requirements of the ATLAS study of five or more tracks associated to a DV.

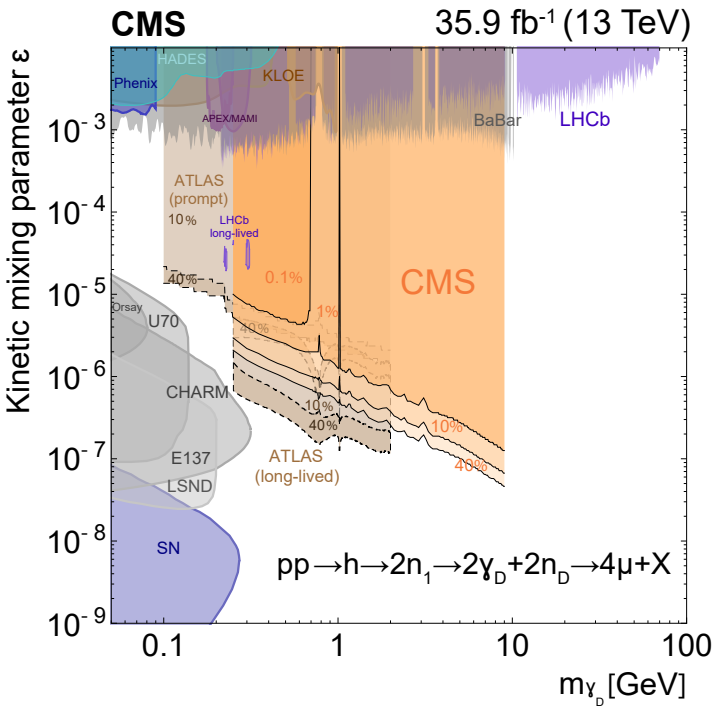

Figure 3.2: Comparison of the lepton-jet searches at ATLAS [265] and CMS [264] with respect to a dark photon scenario [148] vis-a-vis dark photon limits coming from low-energy experiments. Figure taken from Ref. [264].

LLPs) is currently neglected. Furthermore, the sensitivity of the CMS search for two high-$|d_0|$ leptons is currently only sensitive to opposite sign $e\mu$ pairs, with a veto on additional leptons. Relaxing these requirements would greatly enhance sensitivity to certain scenarios, especially the simplified models with flavor-conserving leptonic LLP decays.

Lepton-jet searches currently cover only final states with at least two LLPs and some muons in the final state [13], and the same statement currently applies to both the LHCb searches for dark photons [262, 270] and for LLPs produced in B-meson decays. The existing ATLAS lepton-jet studies express their results in terms of specific dark photon models [14], which makes it complicated to apply the results to other models. We refer the reader to Section 6 for a further discussion of this topic. In extending lepton-jet searches, it would be beneficial to have additional searches with a single lepton-jet or low-mass, leptonically-decaying LLP (which are motivated in models with hidden sectors and Majorana neutrinos, for example in Refs. [43, 128]). In addition, the status of coverage in the intermediate mass-transition region between "standard" displaced lepton pairs and lepton-jets is unclear, and may potentially harbor a gap; adopting the simplified model approach for leptonic LLP decays with masses varying between the GeV and weak scale would ensure comprehensive coverage of low-mass leptonically decaying LLPs.

[13] The ATLAS 8 TeV search [265] included a search channel with two electron-only lepton-jets, but the performance was poor and it was excluded from the final result.

[14] Recall that the lepton-jet studies also consider the $\gamma_D \to \pi^+\pi^-$ decay mode.

Finally, we comment on gaps in sensitivity to very low-mass leptonically decaying LLPs. A benchmark LLP model is the heavy neutral lepton (HNL), which corresponds to the charged-current production mode with (semi-)leptonic LLP decays in our simplified model framework. HNLs constitute an important physics case that leads to multi-lepton displaced signatures from W decays, with nice prospects at ATLAS and CMS (see, e.g., Refs. [43, 47, 48]). While previous searches were not sensitive to this scenario due to either high-p_T requirements or the requirement of two DVs in the same event, the presence of a prompt lepton from the W allows the relaxation of these requirements in a dedicated analysis. Moreover, the prospects of triggering on a prompt lepton in such searches was studied recently in Ref. [47] and demonstrated in a prompt search in Ref. [271] [15]. The identification of two leptons from the vertex is a powerful discriminant against backgrounds from metastable particle decays and hadronic interactions in material. This permits a potentially cleaner exploration of the lower HNL mass range (3–6 GeV) than in the semi-leptonic channel (see Section 3.3) despite the lower branching ratio. It should be noted that HNL models can predict LLP decays to all three lepton flavors (either democratically or hierarchically), necessitating the capability to reconstruct displaced leptons of all flavors, including taus.

[15] Note that the displaced large transverse impact parameter $e\mu$ CMS search [190] fails to cover this scenario due to the aforementioned lepton veto, which eliminates sensitivity to the tri-lepton signals discussed in Ref. [43], as well as relatively high lepton p_T trigger thresholds compared to the kinematics of 4-body W decay.

3.3 *Semi-Leptonic Decays*

As semi-leptonic signatures include aspects of both hadronic and leptonic LLP decays, many of the previously discussed searches can partially cover these cases, and some do so explicitly. For instance, the ATLAS search for electrons and muons accompanied by tracks [189], the inclusive CMS search for DVs [242] (which contains a specific model interpretation called "B-lepton" addressing precisely this channel), and the search for a large impact parameter $e\mu$ pair by CMS [190] are all inclusive with respect to other hadrons produced in the LLP decay, provided the leptons are sufficiently isolated [16]. In addition, LHCb has dedicated searches for semi-leptonically decaying LLPs [272] and semi-leptonic decays of long-lived Majorana neutrinos coming from B^- mesons [273]. The two CMS searches [190, 242] need no further explanation for how they cover semi-leptonic LLPs because of their very inclusive nature (see Section 3.2.1), but we now describe the rest of these searches in some detail.

[16] Note that the lepton isolation affects most of the semi-leptonic searches.

3.3.1 *LHCb Searches*

The LHCb search for semi-leptonic LLP decays selects events with a muon trigger, then reconstructs a DV offline [272]. The results are interpreted in terms of four distinctive topologies: single LLP production in association with a new particle (in this case a gluino), double LLP pair production via direct pair production, Higgs de-

cay, or via squark pair production (heavy parent). The LLP then decays to two quarks and a muon (which maps to the $jj\ell$ simplified model decay). Material regions are vetoed for the DV, which results in the dominant background arising from heavy flavor production either directly or from W/Z decays. The signal discrimination is obtained from a multivariate analysis based on the muon p_{T} and impact parameter, and subsequently the search is optimized based on the LLP reconstructed mass and the muon isolation. This study is sensitive to low-mass LLPs with lifetimes between 1.5 and 30 mm, as can be seen in Figure 3.3.

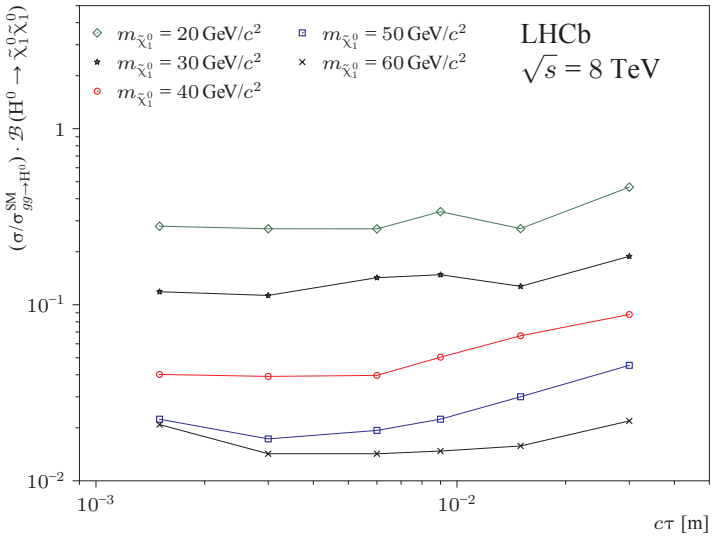

Figure 3.3: LHCb reach for displaced semi-leptonic decays. Taken from Ref. [272].

The LHCb search for Majorana neutrinos [273], N, probes Majorana neutrinos produced in leptonic B decays, $B^{\pm} \to \mu^{\pm} N$. The Majorana neutrino subsequently decays exclusively to $N \to \mu^{\pm}\pi^{\mp}$; both prompt and displaced decays are considered [17]. A same-sign muon requirement, along with the reconstruction of the N and B meson masses, greatly reduces backgrounds to the search. The sensitivity of the search is limited by the restriction to muons in the final state (so models that predominantly decay to e or τ are not constrained), and the same-sign lepton requirement gives sensitivity only to lepton-number-violating processes. More inclusive searches looking for additional N production modes [275], decays with opposite-sign leptons, or searches targeting decays of heavier mesons like B_c [276] could also improve the sensitivity to semi-leptonically decaying LLPs.

[17] Some care is required in interpreting the results of the search on a model with a Majorana neutrino, as the original theory interpretation is problematic [274].

3.3.2 *ATLAS Search*

The ATLAS search for semi-leptonic LLP decays [189] looks for a vertex with a lepton accompanied by tracks. This search uses the same trigger as the dilepton vertex search described in Section 3.2.

The DV is required to have a lepton as well as at least four additional associated displaced tracks, and the invariant mass of the tracks must exceed 10 GeV. Thus, the search in principle can have sensitivity down to masses $\gtrsim$ 10 GeV, although the high p_T threshold for the displaced electron/muon typically limits sensitivity to low-mass LLPs; the vertex must contain a muon with $p_T > 55$ GeV or an electron with $p_T > 125$ GeV.

3.3.3 *Summary*

When considering the application of inclusive hadronic or leptonic searches to semi-leptonic LLP decays, it is important to understand how the simultaneous presence of leptons and jets in the signal can degrade the sensitivity. For instance, prompt jet searches explicitly can remove non-standard jets through jet cleaning cuts. Lepton isolation criteria can severely reduce the signal acceptance for a highly-boosted LLP decaying into a lepton and a jet, and they might also veto extra tracks in the events. Thus, boosted semi-leptonic decays (as might be found in the displaced decay of a low-mass, right-handed neutrino produced via W decay) may not be covered by existing searches.

One of the major gaps in semi-leptonic LLP searches is at the smallest LLP masses. In this case, it can be challenging for the leptons from LLP decays to pass trigger thresholds and/or isolation criteria; backgrounds from heavy-flavor and other processes are also higher for semi-leptonic processes than fully leptonic ones. However, there are very good motivations for low-mass semi-leptonic LLPs from the HNL benchmark model [18] introduced in Section 3.2.5, which predicts LLPs for HNLs of masses below 30 GeV. The signature of HNLs from W decays with displaced semi-leptonic HNL decays is an important item on the search agenda of ATLAS, CMS and LHCb [38, 43, 47, 48, 277, 278]. Recently, there has also been a proposal to search for low-mass HNLs in heavy ion collisions [279]. The semi-leptonic channel has the highest branching ratio (about 50% in the relevant mass range [280]) and can therefore offer the best discovery prospects at LHC experiments for HNL masses up to 30 GeV as long as a DV mass cut of around 6 GeV is made to mitigate backgrounds from B-mesons, $m_B \sim 5$ GeV, and backgrounds from random-crossings can be suppressed. The lower end of the 6–30 GeV mass range corresponds to a non-perturbative regime for the hadronization of the HNL decay products. As the number of charged hadrons significantly affects the DV reconstruction efficiency, the validation of event generator outputs for this process is an important issue currently being addressed by the community (see e.g., Ref. [47]). The ability of LHCb to trigger directly on the HNL decay products and better reconstruct displaced tracks can in some cases compensate for its lower acceptance and luminosity, as exemplified by a recent search for DVs composed of one muon and several tracks [272, 278]; similar

[18] In the language of simplified models, this corresponds to the charged-current production mode, where the HNL LLP is produced in association with a prompt lepton. The HNL then decays semi-leptonically via the $jj\ell$ channel.

arguments can be made in the case of heavy ion collisions [279]. This possibly enables LHCb to better probe the more challenging tau channel. Figure 3.4 shows the overall expected reach of LHC searches in the HNL coupling strength (for the muon channel) versus mass plane, using assumptions detailed in Ref. [277], similar to those in Refs. [38, 43].

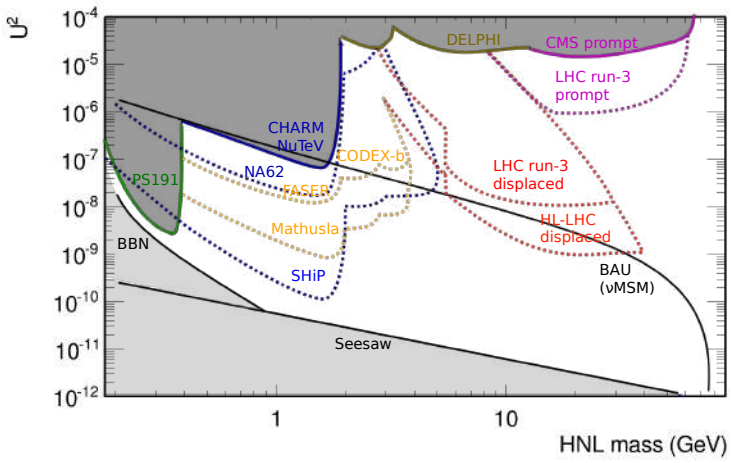

Figure 3.4: Summary of projected experimental sensitivities to HNLs in various experiments, in the coupling strength (U^2 for dominant mixing to ν_μ) vs. mass plane. The projections labelled "LHC Run 3" and "HL-LHC" are for HNLs in W decays in general-purpose experiments, and the one labelled "Mathusla" assumes the full HL-LHC MATHUSLA dataset. We also show the recent CMS result for the prompt tri-lepton signature [271]. Prospects at proton beam-dump experiments are also shown for an already existing experiment, NA62 [281], and for the planned experiment SHiP [282]. Existing constraints from direct searches are indicated as coloured solid lines [283–287]. The lines labelled "Seesaw" and "BBN" show lower theoretical constraints from the observed neutrino masses (assuming a normal hierarchy) and primordial nucleosynthesis, respectively [288]. The line labelled "BAU" is an upper theoretical constraint in the νMSM model for accounting for baryon asymmetry in the universe while the lightest HNL is a dark-matter candidate [288].

The sensitivity of LHC experiments to HNLs is complementary to that of fixed-target experiments which can probe lower couplings thanks to high-intensity beams albeit at lower mass ranges (i.e., targeting HNLs from c and b decays). The CERN SPS provides great opportunities with the running NA62 experiment [289] and the planned SHiP experiment [282], which comprise a vacuum decay vessel and spectrometer tracker downstream of the target to reconstruct vertices of long-lived neutral particles [19]. These provide the best sensitivity to HNL masses up to 2 GeV, where they probe a region of the parameter space favored in models which simultaneously explain neutrino masses, matter-antimatter asymmetry and

[19] The proposed detector FASER would also have the capability to reconstruct such vertices [290].

dark matter [288, 291–293] (see Figure 3.4).

3.4 *Photonic Decays*

There are two ways in which photons coming from LLP decays do not resemble standard photons. First, they cannot be traced back to the PV, thus giving rise to *non-pointing* photons. Second, they can arrive at the ECAL at a time slightly later than expected because the LLP moves slower than the speed of light; these are referred to as *delayed* photons. We note that both kinds of unusual photons can be vetoed in searches for photons that originate from the PV, and thus prompt searches typically provide weaker bounds on LLP scenarios than for promptly decaying signals. ATLAS has a search for non-pointing and delayed photons [294] using the full 8 TeV dataset, which supersedes the 7 TeV analysis [295]. In CMS there are studies for delayed photons in the ECAL [296] and for non-pointing photons detected via their conversion to e^+e^- pairs [297]. The underlying topology in all these models is the neutralino decay into a gravitino and a photon ($\chi_1^0 \to \gamma\tilde{G}$), ubiquitous in gauge-mediated supersymmetry breaking (GMSB) scenarios [50, 298]. Hence all these studies require large $\not{E}_T$ in the final state. This corresponds to heavy parent production of LLPs with decays to a single photon and $\not{E}_T$ in the simplified model framework; all searches described below use the Snowmass Slopes Point 8 benchmark, which is not straightforward to map to a physical spectrum of heavy parent masses.

3.4.1 *ATLAS Search*

The ATLAS study [294] benefits from the capability of the liquid-argon electromagnetic calorimeters to measure the flight direction and the photons' time of flight. Resolutions on Δz_γ, the separation between the PV of the event and the extrapolated origin of the photon, and $|\Delta t_\gamma|$, difference of the arrival time of the photon with respect to the prompt case, are as low as 15 mm and 0.25 ns, respectively. The trigger demands two photons within $|\eta| < 2.5$, with transverse energies E_T of 35 and 25 GeV. In addition, to guarantee the event comes from a proton–proton collision, a PV with five or more tracks with $p_T > 0.4$ GeV is required. The offline selection requires two photons with $E_T > 50$ GeV and $|\eta| < 2.3$, not in the barrel-endcap transition region ($1.37 < |\eta| < 1.52$), at least one of them in the barrel ($|\eta| < 1.37$) and with less than 4 GeV of energy deposited in the calorimeter in a cone of $\Delta R = 0.4$ around them (consituting the *isolation* criterion). In addition, the events are binned in $\not{E}_T$: the $\not{E}_T < 20$ GeV bin contains the prompt backgrounds, the 25 GeV $< \not{E}_T <$ 75 GeV bin is used as the control region, and finally the signal analysis is performed in the $\not{E}_T >$ 75 GeV bin. This study covers lifetimes from 0.25 to 100 ns in the GMSB framework, the lower limit being a hard cut-off imposed

experimentally, as the similarity between background and signal samples in that region makes discrimination rather difficult. The excluded signal rates in this range of lifetimes vary between 0.8 and 150 fb, with the best-constrained value obtained for $\tau \sim 2$ ns.

3.4.2 *CMS Searches*

The CMS study of delayed photons [296] follows a similar approach to ATLAS. The main difference is that it demands only one photon with $p_{\mathrm{T}} > 80$ GeV, but in addition two jets are required. Furthermore, the vector sum of $\not{E}_{\mathrm{T}}$ and E_{T}^{γ}, which is denoted $\not{E}_{\mathrm{T\ nofl}}$, is additionally used for background discrimination. Collisional backgrounds have small $\not{E}_{\mathrm{T}}$ and large $\not{E}_{\mathrm{T\ no}\gamma}$, while the non-collisional backgrounds are characterised by large $\not{E}_{\mathrm{T}}$ and small $\not{E}_{T\ \mathrm{no}\gamma}$. For the signal events the two variables are large, hence they are both requested to be larger than 60 GeV. The time resolution is 0.372 ns, slightly worse than in the optimal scenario of the ATLAS search. Their reach in lifetimes lies in the 2–30 ns range, excluding signal rates of 10–30 fb.

The CMS study of non-pointing photons [297] relies on the photon converting to e^+e^- pairs. It requires two photons, two additional jets, and $\not{E}_{\mathrm{T}} > 60$ GeV. The photon trajectory is obtained from the conversion vertex as the line segment along the momenta of the e^+e^- track pair, and the impact parameter, $|d_{XY}|$, is defined as the closest distance between the photon and the beam axis, which can be determined within approximately 1 mm. A comparison of the reach of these 8 TeV studies, as well as those using the 7 TeV dataset, can be found in Figure 3.5.

3.4.3 *Summary*

The gaps in these studies are straightforward to identify. The requirement of large $\not{E}_{\mathrm{T}}$ is due to the fact that all of these studies have an underlying theoretical picture of neutralinos decaying into gravitinos and photons, motivated from GMSB scenarios. Hence, these searches do not cover cases without the presence of missing energy, including LLPs that decay to $\gamma\gamma$, $l\gamma$ or $j\gamma$. It may be possible to extract a constraint on such LLP decay modes due to mismeasurement of jets or the photon decay geometry which could mimic large missing energy; however, this would be sub-optimal compared to a dedicated search. With the exception of the CMS study [296] which requires two additional hard jets, all of these analyses require two displaced photons. A single displaced photon signature can occur in motivated models: it can easily arise, for example, from a very slightly mixed electroweak triplet and singlet as in SUSY theories (see the UV models in Section 2). Furthermore, as discussed in Section 3.1, a single LLP in the detector can also arise for very large lifetimes of neutral LLPs, which limits the reach of current searches at longer lifetimes. In such scenarios, it is possible that the photons from LLP decay can be quite soft, and obtaining

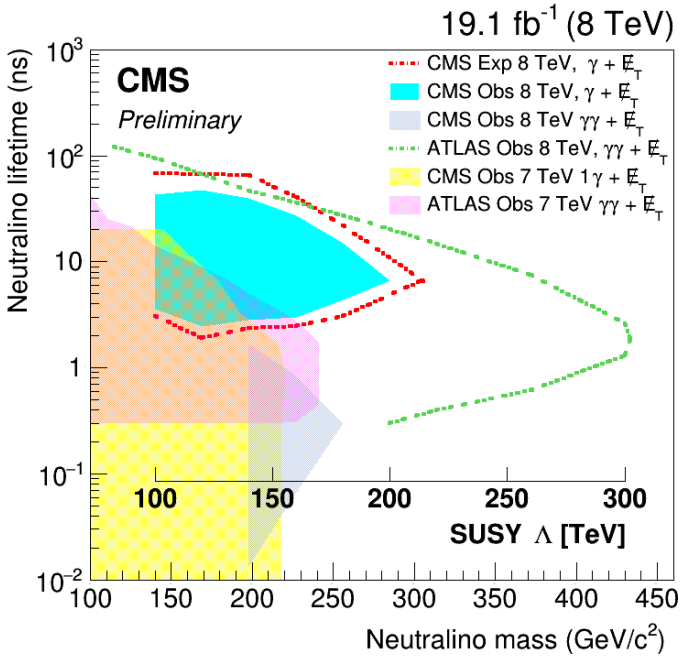

Figure 3.5: Summary of the $\gamma + \not{E}_{\mathrm{T}}$ searches from ATLAS and CMS, displayed assuming the same GMSB model. Taken from Ref. [296].

sensitivity to models with single photons from LLP decay and/or low momenta may require triggering on associated prompt objects, similar to the recommendations in Section 3.1.4.

3.5 *Other Exotic Long-Lived Signatures*

In the preceding sections, we presented analyses sensitive to LLPs decaying into objects such as jets, leptons, and photons. In many cases, however, LLPs give rise to signatures that are completely distinct from more conventional prompt signatures. In this section, we present analyses that exploit properties of other exotic long-lived signatures, such as non-standard tracks. We summarize in detail the existing searches for heavy, stable charged particles (HSCP); disappearing tracks (DT); stopped particles (SP) and monopoles, and describe existing ideas on how to look for quirks and SIMPs (Strongly Interacting Massive Particles).

Note that the terminology employed in some of these searches can be confusing, with occasional conflation of signatures with the underlying model. We provide a detailed explanation of each search, and we attempt a classification here based strictly on signature. We distinguish between three classes of signals: *tracks with anomalous ionization*, *tracks with anomalous geometry*, and finally *out-of-time* decays.

3.5.1 *Tracks with Anomalous Ionization*

In this category, we collect all searches for charged-particle tracks with anomalous ionization, i.e., those that are inconsistent with a charge $|Q| = e$. Here we include i) the so-called heavy, stable charged particles (HSCPs), which apply to stable, electrically charged particles but also charged particles that decay in the calorimeters and/or MS; and ii) magnetic monopoles.

Heavy Stable Charged Particles (HSCPs)

The searches for HSCPs at CMS [4, 299] and ATLAS [216, 300, 301] rely on two key properties. First, particles that are massive and/or electrically charged with $|Q| \neq e$ have a characteristic ionization loss (dE/dx) distinctively different than SM particles. This property can be measured in the tracker. Second, HSCPs are typically heavy and move with a speed less than the speed of light, $\beta = v/c < 1$. Thus, compared to a particle with $\beta \approx 1$, they require a longer time of flight (TOF) to reach the outermost components of the detector (calorimeters and muon chambers). As decays or interactions of the HSCP with the material in the detector can change the electric charge of the HSCP, both CMS and ATLAS perform separate *tracker-only* and *tracker + TOF* studies in the language of CMS [20]. The event selection relies on standard single-muon or large-missing-energy triggers. The offline selection relies on identifying the signal events from quality requirements on the tracks using discriminator variables built from track observables.

[20] ATLAS measures $\beta\gamma$ from dE/dX and β from time of flight and extracts an independent mass, m_β and $m_{\beta\gamma}$, from each measurement.

The HSCP search conducted by LHCb [302] is slightly different. Instead of exploiting dE/dx and time of flight, they use the lack of radiation in the ring imaging Cherenkov detector (RICH). Events are required to pass a high-p_T single muon trigger ($p_T(\mu) > 15$ GeV). Two opposite sign "muons" are then required, each with p_T above 50 GeV and an invariant di-muon mass above 100 GeV, to suppress muons coming from DY production, the main background for this search. In addition, particles must have $\beta > 0.8$, set by the efficiency of the muon chambers to reconstruct slow particles. As electrons and hadrons interact more with the calorimeter than an HSCP, a deposit in the calorimeter of less than 1% of the momentum of the particle is required.

The theoretical interpretation of a signal or limit depends on whether the HSCP carries both color and electroweak charges. If it carries a color charge, the default benchmarks correspond to *R*-hadrons, namely HSCPs that hadronize with SM particles via the strong force, e.g., gluino-gluon or quark-squark states. In the absence of a color charge, the signal is exemplified by long-lived sleptons in the context of gauge-mediated SUSY. Both ATLAS [300] and CMS [4] studies employ these two scenarios, while LHCb [302] uses a stau benchmark model [21]. Finally, CMS also looks for HSCPs coupling only to hypercharge (and hence possessing only couplings to γ and Z), while ATLAS has a search inspired by electroweakinos

[21] The ATLAS R-hadron searches using the 13 TeV dataset have recently been presented in Ref. [216].

in SUSY: it considers the associated production of a neutral and an electrically charged LLP (chargino-neutralino), and thus only one HSCP plus missing energy are required. These scenarios correspond, in our simplified model framework, to the direct production of LLPs with electric or color charges and that do not decay, or decay at very large distances compared to the tracking volume.

To summarize, these searches present no obvious weak points. Standard triggers and tracking algorithms are used, and the analysis methods are well-understood and have been extensively validated against data. HSCP signatures do not suffer from the low-mass gap of many neutral LLPs due to constraints from LEP and other low-energy experiments. However, milli-charged particles are not covered by these searches and require dedicated detectors (see Section 5.3.3). While the HSCP search strategies are generally robust, we encourage the experimental collaborations to continue pursuing improvements for these searches. The small number of signal events that would be produced for HSCPs above current limits render the sensitivity highly dependent on the understanding of the background and control of the systematics.

Magnetic Monopoles

ATLAS [208] has a dedicated search for highly ionizing particles (HIPs), which encompass a variety of new physics scenarios, such as magnetic monopoles, dyons (particles with both magnetic and electric charge), stable microscopic black holes, etc. For the sake of concreteness, we focus on magnetic monopoles but the interpretation in terms of other models is straightforward. [22]

[22] At the time of writing there was no public result on a monopole search from CMS.

The main phenomenological feature is that magnetic charge is quantized in units of $g_D = 2\pi/e \approx 68.5$. Hence, a magnetic monopole behaves as a particle with at least 68.5 electron charges, leading to an unusually large ionization power in matter, so that they would quickly stop in the detector because HIPs lose energy at spectacular rates. Because of the large QED coupling of magnetic monopoles, a perturbative calculation of the cross section is invalid and there is no accurate determination of the production rate, but a naïve Drell-Yan production cross section is provided for the purposes of comparison. The specifics of the detector restrict the sensitivity of this search to magnetic charges $g < 2g_D$ because a large fraction of the monopoles stop in the material upstream of the electromagnetic calorimeter, as the latter is used for the L1 trigger [303]. We note that larger magnetic charges can be tested by the MoEDAL experiment [304], which is described in detail in Section 5.3.2. Additionally, theories with monopoles can also be tested in heavy ion collisions [305].

ATLAS [208] has a dedicated trigger for HIPs based on identifying relevant RoIs in the ECAL and subsequently counting the number of hits in the transition radiation tracker (TRT). As well, the fraction of TRT hits that are high-threshold (HT), meaning that they have an ionization larger than ~ 3 times that expected from a

SM particle, is used as a discriminant. The analysis selects events based on the fraction of TRT-HT hits matched to an EM cluster deposit, and how the energy deposits are distributed in the different layers of the ECAL. It is important to note that due to the lack of a consistent theory, the signal simulation is performed by re-scaling Drell-Yan production at leading order and assuming no coupling to the Z boson. The HIPs are assumed to have either spin-0 or $1/2$. The spin does not affect the interaction with the material, but the angular distributions are different according to angular momentum conservation (keeping in mind that there is, of course, no perturbative theoretical prediction for the angular distribution). Cross section limits for $0.5 < |g|/g_D < 2$ are set for masses in the 890–1050 (1180–1340) GeV range for the spin-0 ($1/2$) case.

The coverage in LHC Run 2 of magnetic monopoles in the $g_D - \sigma$ plane is displayed in Figure 3.6.

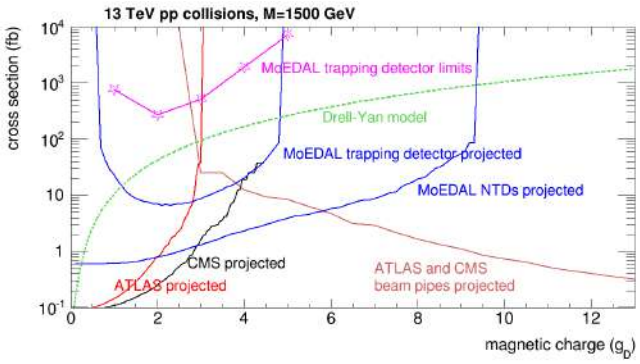

Figure 3.6: Comparison of the MoEDAL, ATLAS and CMS reaches for magnetic monopoles. The curves assume three signal events and a total integrated luminosity of 50 fb^{-1} for 13 TeV collisions [306]. Updated version of existing figure in Ref. [303]. Note that the CMS curve relies on the expected performance of their detector.

3.5.2 *Tracks with Anomalous Geometry*

In this category we group searches where the tracks have an anomalous geometry, namely they disappear (track $\rightarrow$ nothing), or follow non-standard trajectories (such as quirks). There are additional anomalous track signatures that we do not cover such as kinked tracks, where a charged LLP decays to another charged particle that travels at a non-zero angle with respect to the LLP direction [105, 307–309]; however, there are currently no dedicated searches for such signatures.

Within this category we also have the emerging jets signature that has been recently studied by CMS [310]. Since emerging jets arise from dark sector radiation, they are described in detail in Chapter 7 in conjunction with the theoretical and phenomenological aspects of dark showers.

Disappearing Tracks (DT)

Massive charged particles traveling in the detector can decay to a lighter, almost mass-degenerate neutral state, emitting a soft SM charged particle (typically a pion or a muon). While at first glance a small mass gap naïvely seems like a hallmark of tuning, near degeneracies often occur naturally as a result of a symmetry. In fact, electroweak symmetry generically leads to small mass splittings between components of a single electroweak multiplet. For example, $\mathcal{O}$ (100 MeV) splittings arise between the different components of an electroweak multiplet [57, 121] due to EW gauge boson loops [23]. If the SM particle is sufficiently soft it cannot be reconstructed, and then a charged track seems to vanish: this is thus referred to as a disappearing track [24]. The actual lifetime of the charged particle is highly sensitive to the precise value of the mass splitting. For instance, the well studied cases of a fermionic doublet with $Y = 1/2$ and a fermionic triplet with $Y = 0$, reminiscent of a Higgsino and Wino in supersymmetry, respectively, have mass splittings of Δ = 355 and 166 MeV, up to small corrections, but the corresponding $c\tau$ values differ by almost an order of magnitude: 6.6 mm versus 5.5 cm [25]. This is because the lifetime, $c\tau$, depends on the third power of the mass splitting in these scenarios when the charged LLP decays to a charged pion [57, 121].

Before 2017, both ATLAS [311] and CMS [210] required a track to travel about 30 cm in order to be reconstructed, giving good coverage of the Wino scenario. This 30 cm value corresponds to four hits at ATLAS, three in the pixel layers plus one in the silicon tracker, and to seven hits in the pixel and trackers of CMS. The search employs a trigger requiring an ISR jet against which the charged particle recoils, along with the presence of large $\not{E}_{\mathrm{T}}$. The disappearing track is reconstructed offline and needs to fulfill quality criteria (isolation, p_{T} threshold, etc.). A phenomenological study [92] has shown that reducing the distance from 30 to 10 cm would give coverage to the elusive Higgsino scenario, moving the expected reach up to 400 GeV, surpassing the expected mono-jet reach of 250 GeV [312–314]. Later, ATLAS presented a study [211, 315] using 13 TeV data and exploiting the presence of a new innermost pixel layer (IBL). This addition allows for all four hits to be in the pixel, with the outermost pixel layer now at 12.25 cm, enhancing sensitivity to lower values of $c\tau$. The summary for disappearing tracks at ATLAS for the Wino case can be seen in the left panel of Figure 3.7, while in the right panel we show the constraints for Higgsinos from Ref. [92]. CMS also has a disappearing tracks search using 2015 and 2016 data at a center-of-mass energy of 13 TeV [316].

At LHCb the prospects for a disappearing track analysis with the present detector are poor. Currently, the momentum of the track can only be measured if the particle passes through the tracking station (TT), which is about 3 m away from the IP. Particles decaying in the VELO or RICH1 system will not leave a fully-measurable

[23] For a single fermion multiplet, the splitting can only be altered by higher-dimensional operators, and thus it is harder to vary Δ from the 1-loop EW value. For other cases, such as mixing with additional particles, the actual splitting can differ more substantially from this 1-loop EW value.

[24] If the charged particle could be reconstructed this case is often referred to as a *kinked track*. However, as the kinked portion has a very large impact parameter, without a serious attempt to capture the kink these tracks, too, simply disappear.

[25] While these values set a concrete physics target, we stress again that the mass splitting can be arbitrary in other corners of the BSM parameter space (even within SUSY). For instance, $\tilde{\tau} \to \tau\tilde{\nu}$ (where the stau and sneutrino masses are free independent parameters) or for scalar particles (e.g., $H^+ \to \mu^+ H^0$), where the mass splitting and the overall mass scale are set by arbitrary quartic couplings.

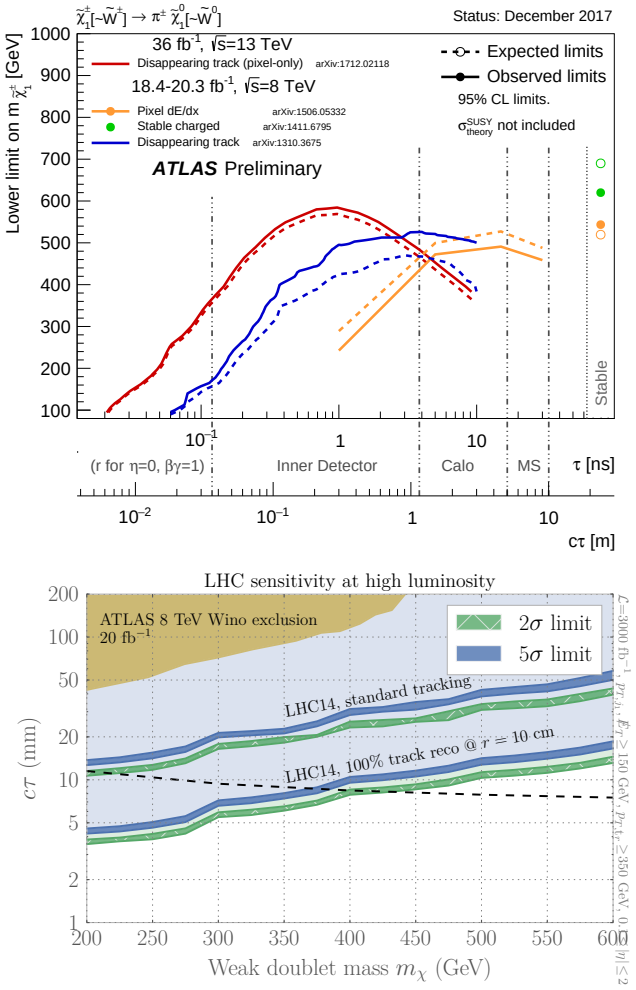

Figure 3.7: **Top:** Summary of ATLAS disappearing-track searches as applied to a Wino (electroweak triplet) benchmark scenario [317]. **Bottom:** HL-LHC projected constraints on the Higgsino scenario [92].

track and will be swamped in a background of SM processes such as kaon decays, which would give a similar signature in the detector components before the magnet. Detector improvements (additional magnets, better PID at low momentum, additional layers) might lead to some sensitivity for $\mathcal{O}$(cm) lived tracks, a golden opportunity for potential LLP discoveries at LHCb in the HL-LHC era.

To summarize, the search for disappearing tracks presents a few challenges. Using an ISR jet trigger means a price is paid in terms of signal efficiency. For example, Ref. [92] has shown that significantly lowering the p_{T} threshold of the jet or directly triggering on the momentum of the disappearing track [26] would lead to a factor of two increase in the number of signal events. It is also clear that better access to lower lifetimes is needed; this may only be possible, for instance, by adding new tracking layers as close as possible to the beampipe (and/or having double layers instead of single ones).

[26] While currently there are some proposals to trigger on tracks [318], those predominantly apply to standard tracks. In particular, the new fast track reconstruction (FTK) system at ATLAS requires 10 hits in inner detector silicon, which corresponds to a decay radius of less than 9 cm. However, pattern banks for hits including high-$|d_0|$ tracks are currently being considered out to $d_0 \sim 2$ cm [319, 320].

Strongly Interacting Massive Particles (SIMPs)

Strongly interacting massive particles (SIMPs) can be motivated by astrophysical observations of dark matter that do not fully agree with the WIMP paradigm (e.g., missing satellites, the core vs. cusp problem; see, e.g., Refs. [321–324] for further discussion). These particles are assumed to interact strongly with baryons. Consequently, the experimental signature is little to no signal in the tracker and the ECAL, and large energy deposits in the HCAL. Such a final state with trackless jets also arises in the context of emerging jets [325], and ATLAS has a trigger for trackless jets in association with a soft muon (where the muon is required to fire L1 of the trigger) [249]. Additionally, the CalRatio trigger and associated search for displaced hadronic decays (addressed in Section 3.1) is designed to be sensitive to a similar signature and could provide some coverage of this signature as well. Strictly speaking, SIMPs are not a track-based signature, but we include them here because the interactions of the SIMPs with the tracker are different from usual hadrons in jets, while the calorimeter signatures are similar.

An LHC phenomenological study of SIMPs was carried out in Ref. [326]. We summarize the main points of the study here. In their setup, SIMPs interact with the SM via an attractive potential (either scalar or vector mediator) coupling SIMP pairs to $q\bar{q}$ pairs. The proposed analysis selects events with high-p_{T}, back-to-back jets within the tracker, exploiting the charged energy fraction within a jet to discriminate signal from background. The astrophysical experimental constraints on this scenario are compared with the expected reach of this search and that of mono-jets in Figure 3.8. Currently there is an ongoing analysis in CMS pursuing this strategy.

Quirks

Quirks are particles charged under both the SM and a new confining gauge group [175], referred to here as "infracolor" (IC). The defining property of quirks is that the tree-level quirk masses m_Q are above the confinement scale Λ_{IC} (and thus similar to QCD but with no light-flavored quarks), so that there is never enough local energy density to create new quirks out of the vacuum. A pair consisting of a quirk and an anti-quirk can live in a quantum-mechanical bound state where the constituents are separated by macroscopic distances $\ell \sim \frac{m_Q}{\Lambda_{IC}^2}$, remaining connected by an infracolor flux tube. The infracolor flux tube exerts a force on each quirk that causes its trajectory to differ from the expected helicoidal ones for SM particles.

The collider phenomenology depends greatly on the size of ℓ. If ℓ is much less than an Å, the rapid emission of infracolor glueballs results in the quirks annihilating before ever reaching the beampipe. For large enough confinement scales, the infracolor glueballs can decay back into SM particles on sufficiently long

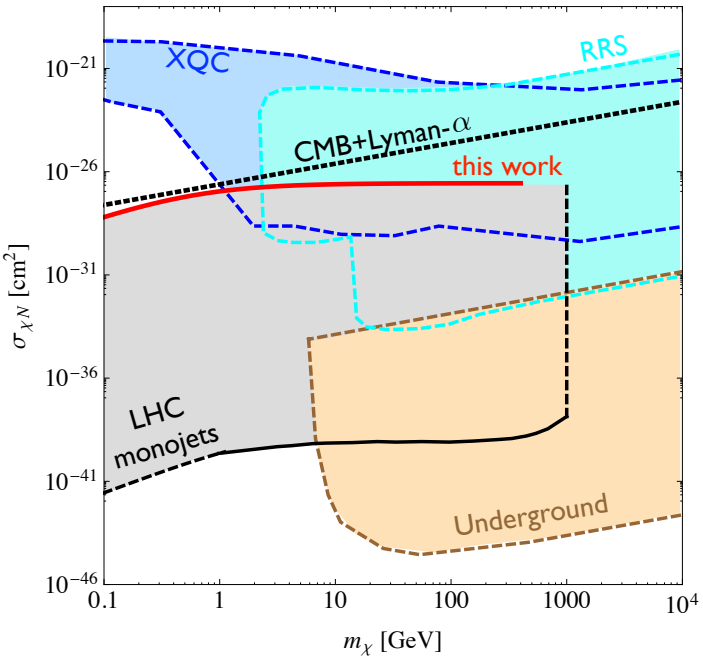

Figure 3.8: Astrophysical and collider constraints on a simple SIMP setup. Note that the relevance of the astrophysical constraints depends on the contribution of the SIMPs to the relic density. Taken from Ref. [326].

.

time scales that they can be distinguished from prompt signatures. While in this specific case, quirks produce hidden valley [59] or emerging jet [325] signatures due to these long-lived infracolor glueballs (see Chapter 7), we stress that elsewhere in parameter space quirks exhibit their own distinct phenomenology and are not merely a subset of hidden valleys, contrary to popular lore.

If ℓ is larger than an Åbut below the mm scale, the individual quirks are not distinguished from one another. However, the pair (which is overall neutral, and therefore does not bend in the magnetic field of the tracker) appears as a single, highly ionizing straight track with missing energy aligned with it, the latter arising from mis-measurement of the track momentum. The *D*0 collaboration has searched for precisely this signature [327], requiring an additional jet for trigger purposes. This search obtained lower bounds on quirk masses of 107, 119 and 133 GeV for SU(2), SU(3) and SU(5) gauge groups, respectively. However, no extensions of this search to higher mass have been performed at the LHC, and the existing HSCP searches require low uncertainties on the track momentum that a straight quirk track would not satisfy.

Conversely, if ℓ is very large then the existence of the confining force has no effect on the quirk motions, and HSCP searches apply directly to the quirk case, with quirks charged under QCD yielding *R*-hadrons and uncolored quirks leading to slepton-like signatures.

We refer the reader to the Section 3.5.1 for more information.

For intermediate values of ℓ, there are interesting phenomenological prospects at the LHC that have been recently studied theoretically [232, 233, 328], but for which there are no current public searches by the LHC collaborations. The first study [232] has recast mono-jet and HSCP searches, finding bounds up to 1.7 TeV for colored quirk masses. In addition, it has also proposed using the CMS dataset taken with zero magnetic field. In this dataset, all SM particles are expected to follow a straight trajectory, but the quirks would still bend due to the string tension. The second study [233] has proposed a new algorithm to search for quirks, exploiting the fact that the quirk and anti-quirk pair should lie in the same plane with the highest sensitivity in the $\ell \sim$ 1-10 mm range. This avoids the necessity of fitting non-helicoidal trajectories, and has the potential to extend the sensitivity to quirks well beyond the current mono-jet and HSCP limits. The third study [328] considers quirks that lose energy through material interactions with the detector. A charged or colored quirk pair can come to a stop within the detector, and annihilate out-of-time with active pp collisions, allowing for sensitivity from stopped particle searches across a wide range of characteristic length scales, $\ell \sim$ Å - km range. We refer the reader to the Section 3.5.3 for more information on stopped particle searches.

Because of the non-standard nature of the tracks, quirk phenomenology poses substantial challenges in their experimental reconstruction, and the lack of constraints on quirks have already attracted the attention of the ATLAS, CMS and LHCb experiments. It would be desirable to test how the phenomenological proposals in Refs. [232, 233, 328], among others, can perform in a realistic detector simulation of one of the LHC experiments.

3.5.3 *Out-of-Time Decays of Stopped Particles*

This category is unique because LLP decays occur out-of-time with the collision. Indeed, decays can even occur when the LHC is not running! The only member of this class is the search for stopped particles (SP), which we describe below.

If an HSCP is produced with very low kinetic energy, it can come to rest in the detector due to interactions with the detector materials. This most likely occurs in the calorimeters or the steel yoke in the muon system as a result of their high material densities. The HSCP can then decay at a later time when no collision is taking place (known as an out-of-time decay). This experimental restriction reduces the types of background processes affecting the search, with the dominant backgrounds coming from cosmic rays, beam halo, and instrumental noise.

In the Run 1 analyses from ATLAS [229] and CMS [227], events are selected with a dedicated trigger selecting bunch crossings which are empty and have no bunches of protons nearby. The anal-

yses require a jet with p_T (E) above 30 (50) GeV at ATLAS (CMS). ATLAS further supplements the hardware trigger by requiring $p_T(j) > 50$ GeV, $|\eta| < 1.3$ and $\not{E}_T > 50$ GeV, rejecting instrumental noise. In addition, CMS has updated the jet search in Run 2 and also provided a search that triggers on out-of-time muons, both of which use the 13 TeV dataset [228]. The latter also employs the displaced stand-alone (DSA) muon reconstruction algorithm [329].

An offline selection procedure is aimed at reducing the main backgrounds. Muons coming from cosmic rays can be identified due to their distinctive topology. The "beam halo" background is the result of protons interacting with residual gas in the beampipe, the beampipe itself, or collimators upstream from the interaction point. Most particles will not travel far before being absorbed by various structures, but muons will travel parallel to the beam and can leave calorimeter deposits out of time with a proton–proton collision. However, these deposits will often be accompanied by corresponding horizontal tracks in the muon systems and can thus be efficiently vetoed. Instrumental noise is rejected in CMS by exploiting the anomalous response in the HCAL.

Stopped particle searches provide an alternative way of probing charged particles besides more conventional HSCP searches. HSCP searches are typically more sensitive to any signature with a charged particle, so stopped particle searches are not often expected to be a discovery mode for most simple new physics scenarios with charged LLPs [27]. The typical added value of SP searches is that they can help identify and characterise positive signals in HSCPs, for instance by providing a cleaner extraction of the lifetime and also to properly identify the decay products. However, in some cases (such as for quirks, where HSCP searches are insensitive in much of parameter space), it has been argued that an SP search could actually be a discovery mode if modifications are made to the search strategy to improve sensitivity to quirks [328]. These modifications that would increase quirk acceptance or lower backgrounds include expanding the η range, implementing higher energy thresholds, using the timing information, and considering shower evolution in the new CMS endcap calorimeter [330].

[27] The reason why the SP searches are less efficient than the HSCP ones is twofold. On one hand, only a fraction of LLPs stop in the detector, while the HSCP search only requires that the LLP crosses the detector. On the other hand, the SP is only looked for in a specific time-window that might fail to catch a large fraction of them.

3.6 *Discovery Opportunities: Overview of Gaps in Coverage*

In the preceding sections (3.1–3.5.3), we have examined the so-called "coverage" of existing searches for LLPs at the LHC with the explicit and express purpose of identifying uncovered realms and places where discoveries could be hiding. Here, we summarize these gaps and potential opportunities for LLP discovery in bullet form, as a to-do list for the experimental community.

1. All-hadronic LLP decays

   - Associated-object triggers (especially motivated by Higgs-like VBF and VH production modes) need to be more comprehen-

sively used to improve sensitivity to low-p_{T} objects.

- Improvements are needed in sensitivity at lower masses & lifetimes (e.g., for LLPs produced in Higgs decays).
- Single hadronic DVs need to be looked for in searches that currently use two (such as decays in ATLAS HCAL and MS).
- Possibilities need to be explored for ATLAS and CMS for online reconstruction of hadronic displaced objects, as the inclusive H_T triggers used by the two collaborations miss these objects unless they have a large p_{T}. (By constrast, LHCb can trigger on a displaced hadronic vertex [246, 247].)
- Low-mass hadronically decaying LLPs can look somewhat like tau leptons, so the question remains as to whether there is any possibility of using, for example, L1 tau triggers to seed displaced jet triggers at HLT and improve trigger efficiency; studies need to be performed by the experimental collaborations.
- The prospects for dedicated searches for displaced hadronic taus need to be investigated, since no dedicated searches currently exist.
- The potential for flavor-tagging displaced jets (b-displaced jets, c-displaced jets, etc) needs to be explored.

2. Leptonic

- Coverage needs to be provided for the intermediate region between boosted, low-mass LLPs (lepton jets) and high-mass, resolved LLPs (resolved ATLAS/CMS searches).
- Improvements need to be made to extend coverage to lower masses and to lower p_{T} thresholds. Currently no prescription or plan for this exists, and so dedicated studies need to be done.
- Searches need to be done for different combinations of charge and flavor of displaced leptons (e.g., same-sign vs. opposite-sign, opposite-flavor vs. same-flavor).
- Searches need to be done for tau leptons in LLP decays, in particular if they come from the ID; an unanswered question remains as to whether displaced-jet triggers can be used for this purpose.

3. Semi-Leptonic

- Searches do not exist and need to be done for LLP masses below about 30 GeV; this mass range is theoretically well motivated by Majorana neutrinos.
- Searches need to be performed for all flavor combinations (for example, one CMS search only covers $e^{\pm}\mu^{\mp}$), as well as same-sign vs. opposite-sign leptons.

- Currently unknown improvements need to be made to relax or modify isolation criteria wherever possible to recover sensitivity to boosted semi-leptonic decays.
- Searches need to be done that better exploit triggering on associated objects for improved sensitivity to low-mass objects, or to employ high-multiplicity lepton triggers if there are multiple LLPs.

4. Photonic
   - There is currently no coverage for LLPs decaying into $l\gamma$, $j\gamma$, or without $\not{E}_{\mathrm{T}}$, and searches urgently need to be performed for this decay topology.
   - There is currently poor coverage (i.e., there exists no dedicated search) for single-γ topologies. The only searches with sensitivity require two jets to be present in addition to $\not{E}_{\mathrm{T}}$ [296]. Studies are needed to assess the sensitivity of this search to signals with only one delayed photon and different jet multiplicities.
   - There is currently no coverage for softer non-pointing or delayed photons, and searches need to be performed for these kinematic realms.
   - Studies need to be performed to determine if triggers on associated objects may improve sensitivity to signals with a single photon, without $\not{E}_{\mathrm{T}}$, or for lower-p_{T} photons
5. Other exotic long-lived signatures
   - Disappearing tracks with $c\tau \sim$ mm are very hard to probe, and new ideas and detector components are needed to extend sensitivity to this potential discovery regime. It's unclear if the ATLAS insertable B-layer will be present in HL-LHC run and how sensitivity to the disappearing track topology will improve with the replacement of the current inner detector with the new ITk (Inner Tracker), or whether new tracking layers very close to the beam line can be added. It's an open question as to what is the lowest distance at which new layers (or double layers) can be inserted. Another open question that needs to be answered is whether there are any prospects for disappearing tracks at LHCb with an upgraded detector.
   - No dedicated searches for quirks exist at the LHC, a huge, open discovery possibility for ATLAS, CMS, and LHCb. Some LHC constraints exist by reinterpreting heavy stable charged particle searches, but dedicated searches need to be performed. There are significant challenges in modeling the propagation and interaction of quirks with the detector, as well as in fitting tracks to their trajectories, but new ideas have been proposed that need to be explored by the experimental collaborations that might allow improved sensitivity to quirks with less ambitious analysis methods.

4
Common Sources of Backgrounds for LLP Searches

Contents

Chapter editors: Juliette Alimena, Martino Borsato, Zhen Liu, Sascha Mehlhase

4.1 Introduction

For many searches for LLPs, the main backgrounds do not stem from irreducible SM processes, but arise instead from *external sources*. Indeed, there can even be backgrounds of instrumental and/or algorithmic nature. Often, LLP searches are designed to have a very small number of background events, sometimes even zero events, that pass the full selection criteria. This chapter gives an overview of common LLP search backgrounds and the means to estimate or control them.

4.2 Long-Lived Particles in the Standard Model

Weak decays of SM particles can naturally give rise to displaced vertices at the boosts typically encountered at the LHC. Searches for LLP signatures at sufficiently low LLP mass and lifetime suffer

from large backgrounds due to displaced SM decays. One simple example is found in the search for long-lived dark photons decaying to $\mu^+\mu^-$ at LHCb [262], which drastically loses sensitivity when the dark photon mass gets too close to the $K_S \to \pi^+\pi^-$ invariant mass, despite the very low $\pi \to \mu$ misidentification rate.

Moreover, b-hadrons can decay at displacements of a few mm and can be challenging to distinguish from LLPs with masses of a few tens of GeV that decay to a pair of jets. Requiring a large track multiplicity of the displaced vertex and performing a mass fit to the dijet invariant mass can help to significantly reduce the effect of this background (see, for example, Ref. [244, 246]). Backgrounds from heavy flavors are typically more abundant in the forward region, as arises, for example, if the signature under study is an LLP from the decay of a SM-like Higgs boson. However, the LHCb forward detector, which was designed to study these SM decays, is, in most cases, capable of rejecting heavy flavor backgrounds more effectively than can be done in ATLAS or CMS. Furthermore, displaced tracks from b-mesons, which usually have impact parameters (d_0) of less than 2 mm, can be rejected by using a larger criterion for the minimum track d_0.

4.3 *Real Particles Produced via Interactions with the Detector*

Particles produced in the pp collision can interact with nuclei of the detector material, giving rise to displaced vertices, and can mimic LLP signals. Vertices from these interactions will be positioned in regions of the detector containing high densities of detector material and are therefore effectively vetoed by using detailed material maps.

The LHC detectors have developed tools internal to the collaborations to define a material volume to be vetoed. As the detector configurations changed slightly from Run 1 to Run 2, material maps have been determined separately for each data-taking period for both the ATLAS and CMS collaborations, using collision data. Maps can be found for ATLAS for Run 1 in Ref. [331], CMS for Run 1 in Ref. [332], ATLAS for Run 2 in Ref. [230], and CMS for Run 2 in Ref. [333]. Additionally, the Run 2 maps for both are shown here in Figures 4.1 and 4.2 for ATLAS and CMS, respectively.

LHCb recently developed a precise material map of the VErtex LOcator (VELO) using beam-gas collisions [334], shown in Figure 4.3. Beam-gas collisions can be distinguished from long-lived heavy flavor backgrounds and their utilization allows the map to cover precisely the whole VELO geometry, not only the region close to the interaction point. This map was used to veto photon conversions to di-muons, which is the main background affecting displaced dark-photon searches at low mass [262]. In analyses, this material map, together with properties of a reconstructed secondary vertex and its constituent tracks, is used to construct a p-value that is assigned to the hypothesis that the secondary vertex

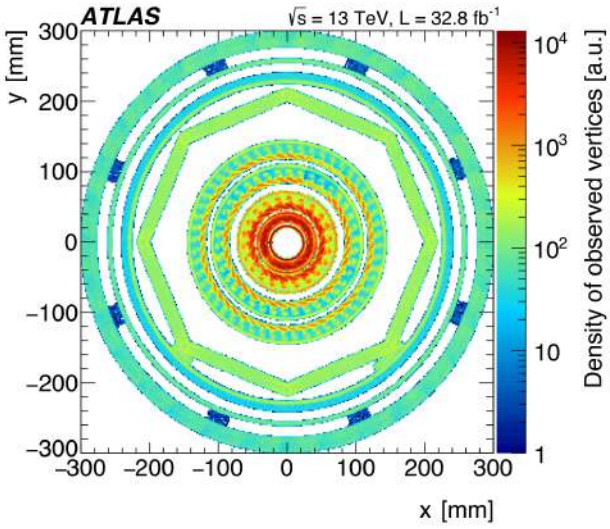

Figure 4.1: An example of a material map from ATLAS [230].

originates from a material interaction. As a rule of thumb, LHCb material interaction background is dominant for vertices at a distance from the beam axis larger than 6 mm (where the VELO material begins). Below 6 mm the background is dominated by heavy flavor decays [335].

Because accurate material maps are essential to performing fully reliable sensitivity studies to signatures with displaced vertices, making them publicly available to the broader LLP community is of the highest priority. The availability of such tools in fast parametric simulations such as Delphes [336] would be very useful to reinterpret LLP search results. In Section 6.4.6.2, an example of a reinterpretation of an LLP search is presented, where a rough material veto was performed because these material maps were not publicly available, highlighting the shortcomings of such approaches in the absence of accurate material maps and emphasizing the benefits of making them available.

High-energy collision muons originating mainly from W decays and creating secondary interactions in the tracker, calorimeters or muon system can be an additional source for displaced vertices mimicking LLP signals. This mostly minor background arises as vetoing these displaced vertices is based on a not 100% efficient detection of the high-p_{T} track in the tracker.

Another important background, mainly for analyses targeting the reconstruction of decay vertices of long-lived particles reaching the muon systems, is hadronic or electromagnetic showers not contained in the calorimeter volume, so-called punch-through jets [241]. These punch-through jets occur especially in regions of reduced total interaction length in the calorimeters (e.g., transition regions between the barrel and the end-caps) and can be suppressed by either rejecting these $|\eta|$ regions or requiring a mini-

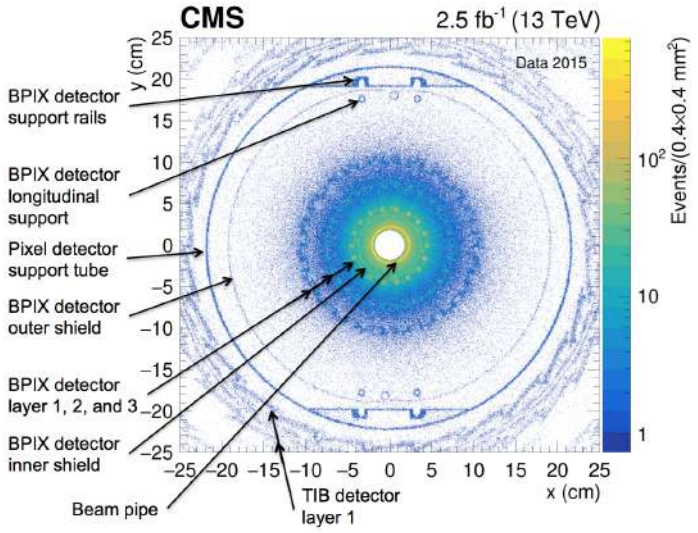

Figure 4.2: An example of a material map from CMS [333].

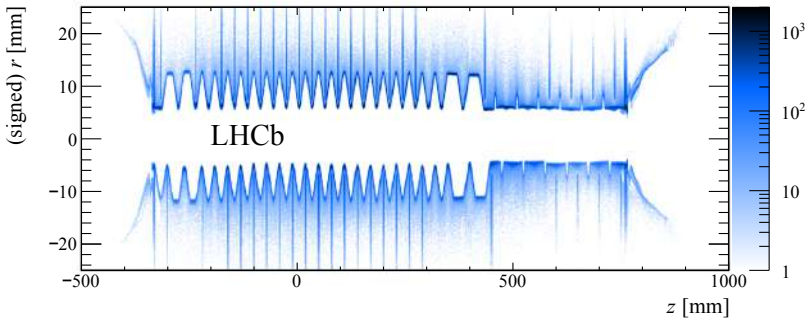

Figure 4.3: Reconstructed secondary vertices in the LHCb VELO from beam-gas collisions in the zr plane integrated over ϕ. These vertices are used to build the material map [334] to veto backgrounds from material interactions.

mal number of hits in the muon system and isolating the displaced vertex from calorimeter jets as well as high-energy tracks and significant track activity in the inner tracking system. In order to not reject true vertices from displaced decays that occur near the end of the calorimeters, the calorimeter-jets veto should only consider jets with a minimum total energy deposit and, e.g., a minimum electromagnetic fraction of the total energy. The track isolation requirement aims at regions with a poor calorimeter measurement (again, transition regions in the calorimeters), where a single high-energy track or the sum of the track activity in a small cone around the displaced vertex could indicate a (punch-through) jet. On the other hand, punch-through jets, given their similarity to signal signatures, can also be used to evaluate systematic uncertainties due to imperfect modeling in the muon-system simulation.

4.4 *Real Particles Originating from Outside the Detector*

There are several types of real particles generated outside the detector that could be sources of background in an LLP search.

4.4.1 *Cosmic Muons*

Cosmic rays from the atmosphere can enter the detector as cosmic-ray muons. These cosmic-ray muons can be reconstructed as displaced muons in the muon system or as displaced jets in the calorimeters. If cosmic-ray muons are reconstructed in the muon systems, they will typically appear as two back-to-back muons with ϕ values near $\pm\pi/2$. The rate of cosmic muons in the detector is about 500 Hz at L1, but depending on the HLT path and the offline selection used, the rate of cosmic-ray muons entering a given LLP analysis is generally much less.

Cosmic-ray muons are typically an important background source to consider for displaced signatures, especially those with large displacements [227, 229, 337–339]. Cosmic-ray muons are generally only an issue for LLP analyses in CMS and ATLAS since LHCb has coverage only in the forward direction.

For many analyses, cosmic-ray muons can be rejected with a simple veto on back-to-back dimuons. However, in some LLP analyses, this veto is not optimal for the signal acceptance or it is insufficient to suppress cosmic-ray backgrounds. Another often-used way to minimize the contribution from cosmic-ray muons is requiring high-momentum muons and/or high-energy jets, since cosmic-ray muons have a rapidly falling p_{T} spectrum. In addition, if a search primarily looks for inner-tracker or calorimeter objects, cosmic-ray-muon events can be rejected by requiring little muon system activity [227, 337, 338].

If the cosmic-ray muon background is significant for an analysis, it can be estimated using data from dedicated cosmic data-taking runs or from empty bunches in pp collision runs [227, 337, 338]. Cosmic ray muon simulations can be made, but in many LLP analyses, a data-driven approach is favoured if the simulation modeling is found to be insufficent. Timing information in the calorimeters or the muon systems can be used to discriminate the signal from cosmic-ray muons, sometimes in conjunction with impact parameter variables.

4.4.2 *Beam Halo*

Another type of real particle generated outside the detector that could be a significant source of background for LLP searches is beam halo. Beam halo is produced when protons from the LHC beam scatter off the LHC collimators and produce debris, which can appear in the detector. Beam halo can create energy deposits in the calorimeters or hits in the muon system, both of which would be largely in the beam direction. These energy deposits or muon

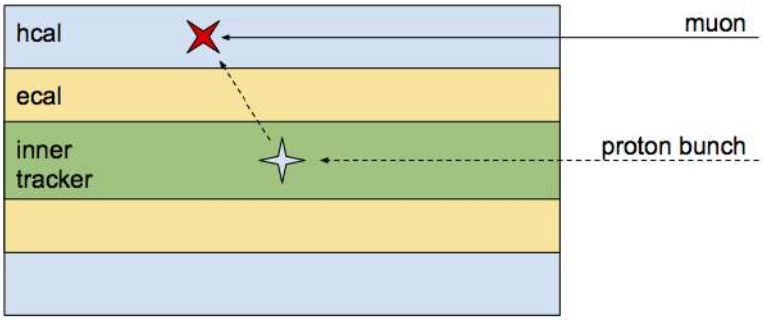

Figure 4.4: A sketch illustrating the timing differences due to the shorter, more direct path to the calorimeter cells between a beam-halo muon and a particle originating from the collision. The beam-halo muon is detected earlier than the particle from the collision.

system hits would appear earlier than if they had been made from particles coming from the collision (see Figure 4.4). Beam halo is usually not modelled in MC simulation, since it is highly dependent on the beam parameters.

Beam halo is most relevant for searches for displaced signatures without tracks in the inner tracker and for searches for decays in non-collision bunches (e.g., from stopped particles) [227, 337, 338], which are described in Section 3.5.

The contribution from beam halo can often be reduced by requiring high-momentum or high-energy reconstructed objects. One can also decrease the number of beam halo events by requiring central objects or vetoing forward muon system activity, since beam halo is usually in the very forward direction [227, 337, 338]. For inner tracker-based signatures, events from beam halo are rejected by requiring a minimum number of early hits; in this way beam halo is rejected due to its anomalous timing.

Beam halo background can be estimated using data control regions near $\phi = 0$ and π. One could also identify cells with a low number of (or zero) tracks that are assigned an early time.

4.4.3 *Cavern Radiation*

Diffuse backgrounds can also arise from proton–proton collisions filling the LHC caverns, consisting mostly of neutral, low-energy, and long-lived SM particles (i.e., neutrons and photons), leading to an overall increase in occupancy, especially in the muon systems. This so-called "cavern background" or "cavern radiation" can constitute a significant background in a LLP search. As simulations are resource-intensive, it is usually not at all modelled in MC simulation samples.

Cavern radiation is most relevant for searches looking in non-collision data, that is, stopped-particle searches, and for searches using muon system information to form tracks and vertices. It can

be estimated from data by collecting events triggered by random triggers when there are no collisions, as was done in Ref. [229]. [1] Cavern radiation can also be estimated by overlaying a cavern radiation simulation with minimum-bias events from data.

[1] Note that these triggers are unlike those used to collect the search data for stopped-particle searches, which instead select events with physics objects during empty bunch crossings.

4.5 Fake-Particle Signatures

Another type of background for LLP searches is that from signatures that mimic real particles in the detector, but are in fact fake. Fake particles can originate from spurious detector noise. Noise appears differently for each detector, but in general, it is characterized by a single and concentrated energy deposit or hit that does not correspond in time or space to any other energy deposits or hits in the detector. Noise is usually difficult to model with MC simulation.

Calorimeter detector noise is most relevant for searches looking in non-collision bunches and low-energy collisions [227, 337, 338]. Muon system noise is most relevant for searches that are also highly affected by cosmic-ray muons.

Calorimeter noise can be rejected by vetoing single and concentrated energy deposits [227, 337, 338]. Muon system noise can be rejected by requiring high-quality muon tracks.

Noise in both the calorimeters and the muon systems could be estimated by looking at dedicated cosmic data-taking runs and then applying some selection criteria to reject cosmic-ray muons. The remaining events would most likely be noise.

4.6 Algorithmically Induced Fakes

For searches that aim to reconstruct the decay vertex of an LLP, and especially for long-lived particles decaying in the proximity of the interaction region, algorithmically induced fakes and/or instrumental backgrounds can be of importance. Algorithmic fakes can still be a significant background to LLP searches, even if a given detector is noise-free.

4.6.1 Random/Merged Vertices

This type of background, illustrated in Figure 4.5, is especially important in the environment close to the interaction region that experiences a high track density, and arises from two main sources. First, two or more individual tracks can cross each other and can be reconstructed as a displaced vertex. Second, two close-by, low-mass vertices can be reconstructed as one high-mass displaced vertex; such a final merging/cleaning step is often part of vertexing algorithms to reduce fakes in standard vertexing.

The former source is mostly suppressed by requirements originally targeting the removal of meta-stable SM particles: a minimum

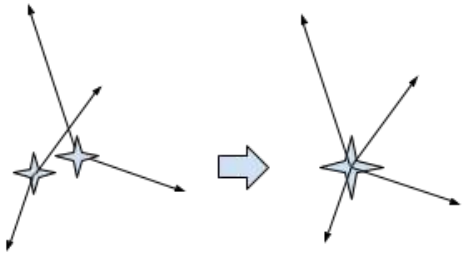

Figure 4.5: Illustration of two close-by, low-mass vertices being reconstructed as one high-mass vertex.

transverse impact parameter, $|d_0|$, for tracks and a minimum distance between the primary vertex and a given displaced vertex.

The latter source is harder to suppress, though can be estimated by randomly merging vertices from distinct events. By studying the number of reconstructed "merged" high-mass vertices as a function of distance between the two low-multiplicity low-mass vertices that were "merged" — both with vertices from the same event, as well as from different events and scaling them accordingly — an estimate for this background can be derived. This method has been successfully used in the ATLAS search for displaced vertices [230] and the ATLAS multitrack analysis [189].

4.6.2 *Randomly Crossing Tracks*

A background that is typically more relevant than merged vertices is the background stemming from low-mass displaced vertices crossed by unrelated tracks, resulting in the reconstruction of a high-mass vertex, as illustrated in Figure 4.6. The mass of the reconstructed displaced vertex is especially increased when the random track crosses the vertex in a direction that is perpendicular to the distance vector pointing from the primary vertex to the displaced one.

As demonstrated in detail in Ref. [189, 230], this background can be estimated by constructing vertices (n-track) from lower-multiplicity ones ($n-1$-track) by adding pseudo-tracks, drawn randomly from data-driven track templates derived for various radial detector regions. The normalization of the prediction is performed by comparing the $n-1$-track-based constructed vertices with the actual n-track vertices in all radial detector regions. One potential method for suppressing such backgrounds is to veto vertices where removing one track substantially decreases the mass of tracks associated with the vertex.

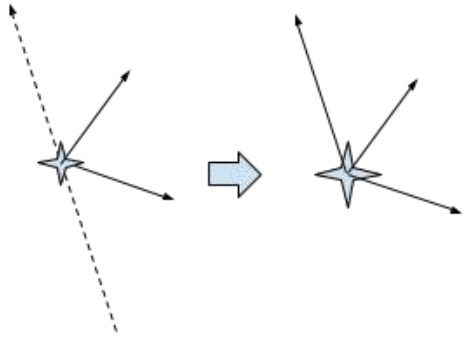

Figure 4.6: Illustration of a low-mass vertex crossed by an unrelated track and being reconstructed as a high-mass vertex instead.

4.7 *Summary*

LLP searches often have very low backgrounds, as opposed to searches for prompt particles. This makes LLP searches highly sensitive to signals of new physics.

There are, however, a few common sources of background that arise in different LLP searches: other, known, long-lived particles such as *b*-hadrons; real particles produced in the detector, such as particles produced in collisions that interact with the nuclei of the detector material; real particles produced outside the detector, such as cosmic muons or beam halo; fake particles, such as detector noise; and algorithmically induced fakes, such as two tracks that cross and are reconstructed as a displaced vertex, as described above. These backgrounds are generally atypical, difficult to model in simulation, and challenging to estimate. Thus, the possible appearance of unexpected background sources should be taken into account in any new LLP search, and the development of novel techniques and methods to estimate them is encouraged.